U.S. Fish & Wildlife Service

Humboldt Bay National Wildlife Refuge

Climate Inventory and Summary

By Rachel Esralew and Sarah Michehl, Hydrologists, Pacific Southwest Region Inventory and Monitoring Program

U.S. Department of the Interior

U.S. Fish and Wildlife Service

Executive Summary

The purpose of this report is to summarize existing and observed trends in temperature and precipitation patterns and forecast climate change projections near the Humboldt Bay National Wildlife Refuge (HBNWR), and to summarize literature on sea level rise in relation to abiotic threats to refuge ecosystems . This report is in support of a Natural Resources Management Plan (NRMP) for the refuge.

The mean monthly temperature near HBNWR from 1984 to 2013 ranged from 41.1 to 61.4 °F with minimum temperatures in January and December and maximum temperatures in August. Mean total water year precipitation near HBNWR was 38.4 inches per year (ranging from 20.7 to 58.8 inches per year) near the refuge. Precipitation was higher for inland areas, with a mean total water year precipitation of 45.7 inches per year.

One might expect a greater likelihood of warmer conditions near HBNWR during El Niño, the warm phase of Pacific Decadal Oscillation, and positive phase Pacific North American pattern. Precipitation was not statistically correlated with any global teleconnection index.

Historically (1910-2014), temperature has already increased over many seasons and months over several time periods tested, but only cool season maximum temperatures near HBNWR continued to show increasing trends after 1985 through 2014. Increases in cool season temperatures were relatively small and ranged from 1.3 to 2.4 °F over the time periods tested.

Some decreases in annual and cool season precipitation were observed in inland areas, however, precipitation has generally stabilized since 1985 at all locations. Median decreases in annual precipitation in the Humboldt Bay drainage basin or inland from HBNWR ranged from 10.1 to 10.6 inches over the period 1950-2013 (.15 to .17 inches per year respectively).

Within and near HBNWR, changes in 30-year forecasts for precipitation and recharge (values were uncertain among models, showing either decreases or increases by 2100. Changes in mean 30-year precipitation at HBNWR and within the Humboldt Climate region of hydrologic influence (RHI) ranged from -17.9 to +31.5 percent (-9.8 to 17.3 inches) respectively.

Maximum and minimum temperature increased under all model and emission scenarios through 2100 (figure 15). By 2100, increases in maximum temperature ranged from 3.8 to 7.8 °F, while increases in the mean minimum temperature ranged from 4.1 to 7.1 °F.

Water demand increased under all model and emission scenarios through 2100. By 2070–2100, Climatic water deficit (CWD) increases showed an 11.9 to 19 percent increase in water demand required over the refuge to support refuge natural resources/ecosystems..

A previous study showed that sea level has already risen from 0.1 to 0.23 inches per year within and near HBNWR. Rates of subsidence were measured to range from -0.01 to – 0.14 inches per year, which exacerbate the impact from rising sea levels.

Sea levels north of Cape Mendocino (12 miles south of the Humboldt Bay spit) are projected to change -1.6 (sea level fall) to +9 inches (sea level rise) by 2030, 12 inches by 2050, -1 to 18.9 inches by 2050, and 3.9 to 56.2 inches by 2100.

Background

Humboldt Bay National Wildlife Refuge was established in 1971 to conserve natural resources that benefit a diversity of birds, mammals, fish, amphibians, invertebrates, and plants that occur in the Humboldt Bay area in northwestern California. The refuge has several management units totaling 9,502 acres (3,379 acres in fee and title). These units consist of a mosaic of mudflats, estuarine eelgrass meadows, salt marsh, brackish marsh, seasonally flooded freshwater wetlands, riparian wetlands, streams, coastal dunes, and forest (U.S. Fish and Wildlife Service, 2005).

The refuge manages its natural resources through a variety of restoration and enhancement projects, including direct management of water levels, vegetation and soil conditions. Much of the historic tidal marsh that once occurred within HBNWR has been significantly modified by human actions such as diking, filling, and agricultural conversion. Refuge efforts have focused on restoration of these areas to increase wetland functionality, including removal of dikes, management of tidegates to permit estuarine influence and allow passage of fish in muted tidal systems, use of water control structures to manage water levels and flow rates in seasonal wetlands, restoration of historic stream channels, and soil modification and filling of subsided areas to promote re-establishment of vegetated wetlands (U.S. Fish and Wildlife Service, 2005).

The Natural Resources Management Plan (NRMP) for HBNWR is designed to support strategic and adaptive management of refuge priority natural resources of concern (hereafter referred to as 'conservation targets'). Refuge conservation targets are riparian forests and swamp, managed marsh (freshwater permanent and seasonal marsh, and brackish marsh), muted tidal sloughs and creeks, salt marsh, tidal flats and sloughs, and eelgrass. Each of these conservation targets has one or more associated 'nested targets' such as Aleutian Canada geese, Pacific brant, rare salt marsh plants and federal or state listed species (e.g., salmonids, tidewater goby).

The process to establish an NRMP includes evaluating threats to refuge conservation targets, including climate change (G. Block, Pacific Southwest Region Inventory and Monitoring Specialist, oral communication, October 2014). Climate change has the potential to negatively impact refuge biodiversity and operations in a variety of ways. A rise in relative sea levels may reduce the extent of the tidal marsh ('marsh drowning') or result in conversion of existing freshwater and brackish wetland ecosystems (e.g., to tidal mudflats via levee failures). Alterations in the timing and magnitude of freshwater inflows, as a result of changes in precipitation and temperature patterns, could impact several aquatic ecosystems of the refuge (e.g., freshwater and seasonal wetlands).

The purpose of this report is to summarize existing and observed temperature and precipitation patterns and trends near the refuge and in an area of interest or influence to refuge resources. This includes 1) a summary of recent averages in temperature and precipitation, 2) an analysis of correlation between temperature and precipitation and larger global teleconnection indexes, 3) historic trends in temperature and precipitation, 4) projections of temperature and precipitation under selected global climate models and a variety of climate change scenarios, and 5) literature summary of the abiotic impacts of sea-level rise.

Methods

Identification of Hydrologic Data Used in Summary

Identification of Spatial Boundary Conditions to Inventory Hydroclimate and Hydrologic Monitoring Data

All climate stations that provided data for this report were selected by defining a region of hydrologic influence (RHI) for HBNWR. The purpose of an RHI is to represent an area of similar climate or hydrologic conditions as the refuge, and to select areas that likely have an influence on surface water conditions at the refuge. Sub regions within the RHI are referred to in the remainder of this section as the climate RHI or surface water RHI. The climate RHI represents an area with similar or representative climate conditions as the refuge and surface water RHI. The surface water RHI represents the area that drains freshwater runoff to the refuge boundary.

The climate RHI was estimated by conducting a spatial cluster analysis of 30-year mean temperature and precipitation from the Parameter-elevation Regressions on Independent Slopes Model (PRISM; PRISM Climate Group 2014, see description of dataset in later sections). The Iso Cluster tool was used in Arc 10.1 (ESRI, 2012) and run with a Maximum Likelihood Estimator to assign distinct classifications among groups of cells in the input rasters (30-year mean temperature and precipitation). This clustering was used to select areas of similar temperature and precipitation as the refuge within a selected area (boundary mask). A boundary mask is defined as the boundary limits where spatial clustering is performed. For example, if the clustering is done for 3 classifications within the boundary mask, Iso Cluster identifies three statistically distinct groups of cells within the boundary mask. The boundary mask was set as the Level 3 Ecoregion (Marine West Coast Forest, Griffith et al. 2008). A maximum of 3 possible classifications were calculated throughout the selected area. The cluster of statistically similar cells that encompassed the refuge was then intersected with a 20 mile buffer from the refuge to select a relatively local area to the refuge. Lines were generalized manually to create a polygon to represent the climate RHI (figure 1).

The surface water RHI was selected as the HU-12[1] drainage basin that encompassed all freshwater drainages that reached Humboldt Bay. HU-12 was derived from the U.S. Geological Survey National Hydrologic Dataset (U.S. Geological Survey, 2015). For the remainder of this report, the surface water RHI is referred to as the "Humboldt Bay drainage basin".

Inventory of Hydroclimate and Hydrologic Monitoring Data

All climate monitoring stations that provided data for this report were selected within the climate RHI boundary described above. Monitoring station locations and data were referenced and obtained using only publicly available internet sources (appendix B, table B1) and refuge archival records. Available data from selected monitoring stations were used to characterize recent hydrologic conditions and to assess trends. If monitoring station information for the same station was provided on more than one database or server, then a decision was made: if a server provided more easily accessible location information or hydrologic data, or included a longer period of record for that station, then that server was selected. Not all data from stations

[1] Within the Watershed Boundary Dataset, the United States is divided and sub-divided into successively smaller hydrologic units. The hydrologic units are arranged or nested within each other, from the largest geographic area to the smallest geographic area. Each hydrologic unit is identified by a unique hydrologic unit code (HUC) consisting of two to twelve digits based on levels of classification in the hydrologic unit system. The higher the code digit, the smaller the watershed unit. 12-digit hydrologic units represent the smallest watershed sub-division in the hierarchy of hydrologic units (Seaber et al. 1987)

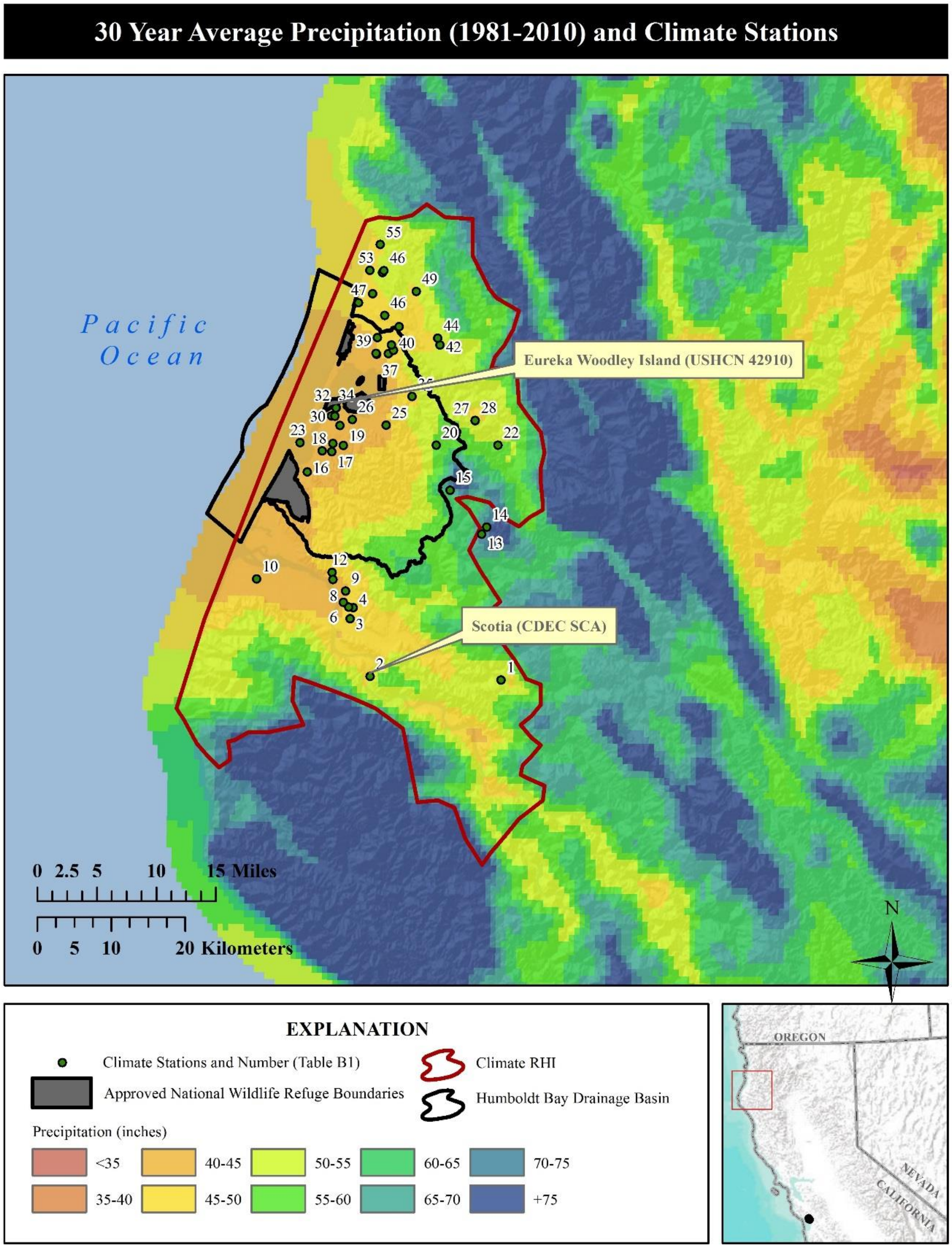

Map Projection: North American Datum 1983 Universal Transverse Mercator Zone 10; Map Production Date: December 19, 2012, Edited September 24, 2014; Source Data: Precipitation Grid from PRISM Climate Group;Terrain from ESRI Online Map Services; Refuge and county boundaries from U.S. Fish & Wildlife Service Cadastral Data, November 2014; RHI, Region of Hydrologic Influence

Figure 1. Mean annual precipitation, inventoried climate stations, and selected regional boundaries near Humboldt Bay National Wildlife Refuge. Eureka Woodley Island and

Scotia climate stations were selected to perform long-term trend analysis of temperature and precipitation at the refuge.

inventoried as shown in appendix B table B1 were used in this report because some stations' periods of record were too short to identify trends or to describe hydrologic variability (as described in later sections). However, omitted stations are identified in this report for potential use in other assessments.

Climate monitoring stations were inventoried to determine which stations provided data that represented climate conditions in the climate RHI. Sources of climate station information included the California Irrigation Management Information System (CIMIS; California Department of Water Resources 2015a), Integrated Pest Management Program California Weather Database (University of California–Davis 2015), U.S. Historical Climatology Network (USHCN, Easterling et al. 2009), California Data Exchange Center (CDEC; California Department of Water Resources 2015b), the Global Historical Climatology Network (GHCN, National Oceanic and Atmospheric Administration 2015a), and MesoWest Climate Data Portal (University of Utah 2015). Fifty-five climate stations within the climate RHI were located (figure 1; appendix B, table B1); these were found through MesoWest Climate Data Portal, CDEC, IPM, USHCN, and GHCN (appendix B, table B1). No CIMIS stations were found in this area.

Modeled Hydroclimate and Hydrologic Data

Additional geospatial models were used to supplement information from stations or to account for variation in parameters over space. The two main geospatial models used to supplement monitoring station information in assessing water resources for HBNWR were PRISM and the Basin Characterization Model (BCM; Flint and Flint 2012).

The PRISM model was used to map 30-year mean precipitation for the region surrounding the refuge and was used to characterize recent conditions in selected subbasins within the Humboldt Bay drainage basin. PRISM is an analytical model that uses climate monitoring data, a digital elevation model (DEM; topography and orographic features), and atmospheric characteristics to generate estimates of monthly and annual precipitation and temperature (PRISM Climate Group 2014). To assess long-term trends in temperature and precipitation in the Humboldt Bay drainage basin, PRISM raster layers were clipped to this area, and 800-meter monthly PRISM raster grids were compiled for the period 1910–2014 using a script called the Refuge Climate Assessment Tool (E. Holmes, Faculty, University of California Davis Center for Watershed Sciences, digital communication January 2014) developed for the R statistical program (The R Project for Statistical Computing 2014).

BCM was used to project effects of climate change on temperature, precipitation, climatic water deficit (CWD), and groundwater recharge. BCM is driven by high resolution (270-meter) temperature and precipitation data downscaled from PRISM that is used to characterize water budget at the land surface. Calculation of variables associated with water budget incorporates static inputs (elevation, bedrock properties, soil properties), and downscaled or modeled time variable inputs (precipitation/snow, temperature, derivatives from solar radiation) to produce water budget outputs (CWD,[2] runoff, recharge) for current conditions and forecasted for a range of climate change scenarios (Flint and Flint 2007). As part of CWD, potential evapotranspiration (PET)[3] is the total amount of water that can evaporate/transpire given temperature, solar radiation, and other variables. Actual evapotranspiration (AET), which is used to calculate CWD, is controlled by soil characteristics (porosity, field capacity, wilting point, and infiltration to bedrock) (Flint and Flint 2007).

Analysis Methods for Climate

Characterization of Climate Conditions

To evaluate existing climate characteristics relevant to HBNWR, climate station information and PRISM data were summarized to estimate precipitation, temperatures, and evapotranspiration conditions that affect the refuge. In general, climate data were used to assess the following near the refuge:

- range of observed daily and monthly temperatures
- range of observed monthly and annual precipitation
- comparison of both temperature and precipitation near the refuge and in the Humboldt Bay drainage basin

Two climate stations were selected for analysis of recent conditions. The Eureka Woodley Island station (station 33, figure 1; USHCN station 42910) was selected for analysis of temperature and precipitation conditions near the refuge. This station was optimal for estimating climate conditions at the refuge because the period of record was 1878–present; although only 1910-present was used to align with the period of record for PRISM data). The Scotia climate station (station 2, figure 1; CDEC Station SCA) was selected to evaluate precipitation farther inland because of the substantial variability of precipitation records across the study area (figure 1).

To plan for effective water management, an understanding of the expected inter-annual variability of climate, or climate predictability, is required. Climate change may pose further uncertainty regarding this variability; however, a baseline understanding of the

[2] CWD is the difference between PET and AET and represents the amount of additional water that would have evaporated or transpired had it been present in the soils (Flint and Flint 2007). Negative values indicate water storage.

[3] Reference evapotranspiration (ETo), measured at CIMIS stations, more closely resembles PET than AET because it is measured primarily from climate factors (solar radiation, humidity, vapor pressure, air temperature, and wind speed), but unlike AET, it does not take into account the ability of underlying soils to store or transmit water to recharge or the atmosphere. Differences in modeled PET and ETo likely occur because a reference crop is not defined in PET and because weather data measured at a station in which ETo is estimated are typically collected from a well-defined reference environment (well-irrigated and well-maintained grass area). ETo can be measured accurately only at the climate station; accordingly, PET is used to estimate PET over large areas. For this reason, PET is more useful than ETo for comparing water demand between areas.

current variability in climate conditions that affect the refuge can help evaluate future impacts associated with the magnitude, frequency, and duration of climate conditions.

An understanding of global climate factors and large-scale circulation patterns that influence the variability of temperature and precipitation at a scale relevant to refuge water resources is useful for understanding climate predictability. Numerous studies have examined the use of global teleconnection[4] indices that indicate the effect of these large-scale circulation patterns on local climate (temperature and precipitation).

For example, the El Niño–Southern Oscillation (ENSO) phenomenon[5] as indicated by the Southern Oscillation Index[6] (SOI), is related to precipitation, snow accumulation, and streamflow in western North America (Cayan et al. 1998; Francis et al. 1998). During El Niño, the southwest tends to be wet and the northwest tends to be dry (negative SOI)—and conversely so for La Niña (positive SOI) (Dettinger et al. 1998). Redmond and Koch (1991) showed that October–March precipitation was most strongly correlated with SOI averaged over the July–November period.

Another teleconnection index commonly analyzed is the Pacific Decadal Oscillation (PDO),[7] which is related to precipitation and temperature. Gershunov and Barnett (1998) demonstrated that when PDO and ENSO are in phase (El Niño—warm PDO; La Niña—cold PDO), the ENSO climate signals described above are stronger and more stable with regard to winter precipitation in the western United States, whereas out-of-phase relations between PDO and ENSO have a weaker climate signal.

The Pacific North American teleconnection pattern (PNA) is one of the most recognized, influential climate patterns in the Northern Hemisphere mid-latitudes beyond the tropics. The positive phase of the PNA pattern is associated with above-average temperatures over western Canada and the extreme western United States, and below-average temperatures across the south-central and southeastern U.S. The positive phase correlates to a pressure ridge over the western U.S., which correlates to drier conditions. The negative phase correlates to below average temperatures for the western U.S., and possibly more storms. The PNA tends to have little impact on surface temperature variability over North America during summer (National Oceanic and Atmospheric Administration, 2015c). Redmond and Koch (1991)

---

[4] Teleconnection indices are used to measure patterns in teleconnections, which refer to recurring and persistent, large-scale patterns of pressure and circulation anomalies that span vast geographical areas. Although patterns can last for weeks and months, they can occasionally be prominent for several years, which reflect interannual and interdecal variability of atmospheric circulation. Teleconnection indices are used to normalize teleconnection patterns so that patterns and trends can be better measured and understood (National Oceanic and Atmospheric Administration 2015b).

[5] El Niño is an oscillation of the ocean temperatures in the equatorial Pacific that has implications for global weather. El Niño is characterized by unusually warm ocean temperatures, whereas La Niña is characterized by unusually cool temperatures in the equatorial Pacific (National Oceanic and Atmospheric Administration 2015b).

[6] The SOI is an index that combines the Southern Oscillation (differences in ocean temperatures in the equatorial Pacific) and is computed as monthly mean sea level pressure anomalies at Tahiti and Darwin (National Oceanic and Atmospheric Administration 2015c).

[7] The PDO is a pattern of Pacific climate variability that shifts phases on an inter-decadal scale (20–30 years) and is detected as warm or cool surface waters in the Pacific Ocean north of 20 degrees latitude (National Oceanic and Atmospheric Administration 2015d).

found that the PNA pattern was directly related to precipitation and temperature, and noted especially strong associations in the Pacific Northwest.

Precipitation and temperature data from the Eureka Woodley Island climate station, Scotia climate station, and PRISM monthly averages for the Humboldt Bay drainage basin were compared with SOI and PDO to determine if these teleconnections were strongly linked to temperature and precipitation affecting the refuge and whether these teleconnections can be used to predict climate characteristics at and near the refuge.

A Kruskal–Wallis test[8] was used to compare the distribution of cool-season precipitation (October–March, as percent above mean) and temperature (average annual in degrees Fahrenheit [°F]) to the distribution of SOI (July–November) and PDO (October–March). SOI was divided into phases of El Niño years (SOI of less than or equal to -0.5), neutral years (SOI between -0.5 and 0.5), and La Niña years (SOI greater than or equal to 0.5). PDO was divided into phases of warm years (PDO greater than 0.5), neutral years (PDO between 0.5 and -0.5), and cool years (PDO less than -0.5). Temperature and precipitation values for each year were assigned the teleconnection categories listed above based on the corresponding year. The Kruskal–Wallis test was run to compare more than one distribution in multi-distribution groups to determine which distributions were different. Results of the Kruskal–Wallis test are presented as a table in this report. A boxplot was developed to show differences in the distributions of temperature and precipitation between teleconnection groups.

Estimation of Trends in Response to Climate Change and Anthropogenic Stressors

To evaluate existing precipitation and temperature trends as a result of climate change, time-series trends in annual and seasonal precipitation and temperature were evaluated for the Eureka Woodley Island climate station, Scotia climate station (precipitation only), and monthly average PRISM clipped to the Humboldt Bay drainage basin. Long-term data (1910–present) were available for these locations, and were representative of the study area. Time-series were generated from monthly precipitation (total inches) and monthly temperature (maximum, minimum, and range of difference between maximum and minimum) for the following aggregated time-periods: seasonal (four seasons), cool-season (October–March), and annual. In addition, time-series were generated for precipitation and temperature (range of difference between maximum and minimum only) for 12 separate months.

---

[8] The Kruskal–Wallis test was used to compare multiple datasets simultaneously to determine if the locations of distributions among all groups were statistically different at a p-value of 0.05.

The Kendall's tau statistical time-series trend test was run to test whether all time-series trends were statistically significant at a p-value of 0.05 (Sen 1968; Dietz 1989; Kendall and Gibbons 1990) and compute the Sen slope.[9]

Because the Kendall's tau statistical test is used to estimate the presence of a monotonic trend (singular direction with time), smaller scale shifts (shifts in climate within the period of record tested) in climate may result in signal noise that precludes accurate detection of trends over a long period of time (Helsel and Hirsch 2002:323–334). To determine which parameters had the most persistent trends (trends that remained significant and in the same direction for variable time periods over the period of record), the following time-periods were tested: 1910–2013, 1925–2013, 1950–2013, and 1984–2013 (last 30 years).

Climate change projections for temperature, precipitation, PET, CWD, and recharge within the refuge boundaries were modeled by comparing four climate change scenarios overlayed with BCM model inputs and outputs by comparing mean conditions for 1971–2010, 2010–2039 (near future), and 2070–2099 (distant future). Climate change scenarios were modeled in BCM using six different General Circulation Models (GCMs): Geophysical Fluid Dynamics Laboratory (GFDL) model, Model for Interdisciplinary Research on Climate (MIROC Medres), Beijing Climate Center China Meteorological Administration Model (BCC_CSM), Bergen Climate Model Version 2 (BCCR_BCM2), Parallel Climate Model General Circulation Model (PCM), and the Commonwealth Scientific and Industrial Research Organization (CSIRO).

GCMs were selected to represent a range of projected precipitation and air temperature conditions spanning from warm and wet to hot and dry. These six models were selected with varying levels of change in precipitation and temperature from historical to potential future conditions, with the purpose of selecting distinct climate scenarios.

All models were run using medium to high carbon dioxide emissions or medium to high increase in carbon dioxide concentrations; all models were run using the A2 emissions scenario,[10] with the exception of BCC_CSM which was run under the similar RCP6.0[11] carbon concentration scenario (Flint and Flint 2012).

Climate change will result in global sea level rise that could ultimately affect flow dynamics in coastal estuaries, sloughs, and drainage basins. A literature review of known

---

[9] Kendall's tau test is a non-parametric statistical test that can be used to indicate the likelihood of upward or downward trends in data with time. Tau coefficients range from -1.0 to 1.0; a tau of -1.0 indicates that every datum decreased with time, and a tau of 1.0 indicates that every datum increased with time. A trend slope is a measure of trend magnitude that was computed using the Sen slope estimator. The Sen slope is estimated by computing the median of all slopes between each possible data pair in the time-series (Sen 1968).

[10] Several families of emission scenarios are discussed in the International Panel on Climate Change's fourth assessment report. Scenario A2 is the carbon emissions in a differentiated world and is characterized by self-reliance in terms of resources and less emphasis on economic, social, and cultural interactions between global regions. Economic growth is uneven, and the income gap between now industrialized and developing parts of the world does not narrow (Solomon et al. 2007).

[11] Representative Concentration Pathways (RCP) are four greenhouse gas concentration trajectories adopted by the International Panel on Climate Change for its fifth assessment report (Richard et al. 2008). Each trajectory represents a possible range of radiative forcing values in the year 2100 relative to pre-industrial values.

impacts of sea level rise in the Humboldt Bay region was performed to evaluate climate change as a potential threat or change to refuge habitats and infrastructure.

Climate Inventory and Summary

Hydroclimatic Settting

Meteorological conditions in northern coastal California are predominantly determined by the north Pacific high pressure system. HBNWR is located on the eastern edge of this system (Ruffner 1985). Large-scale subsidence (areas where large masses of cooler, drier air descend from higher to lower elevations, causing an increase in barometric pressure), which occurs over the subtropical regions, is the major cause of the north Pacific high pressure system (Nuss 2014).

In May–October, storms generally progress in a northerly direction to the California coast because the north Pacific high pressure center moves north from subtropical regions. As a result, there is little to no rainfall in the summer (Ruffner 1985). In the winter (November–April) this pressure system moves southward which allows storm centers to move into California (Nuss 2014). The majority of rain falls during the winter season due to the increasing presence of mid-latitude storms.

The coastal zone and inland areas of Humboldt County are characterized by a Mediterranean climate with heavy precipitation and cool temperatures from October through April, and drier moderately foggy conditions in summer (U.S. Fish and Wildlife Service, 2005). HBNWR experiences maritime climate conditions with high humidity year-round. Winds prevail from the northwest during spring and summer. Winter storms can bring heavy winds as high as 60 miles per hour, generally from the south or southwest (Western Regional Climate Center 2008). During the drier season of May through September, morning fogs are frequently observed which typically dissipate by the afternoon.

The Palmer Drought Severity Index (PDSI) responds to long-term weather conditions and provides a coarse-level indication of regional meteorological wet or dry periods (National Center for Atmospheric Research 2013, figure 2). The index uses 0 as a normal, dry years are represented as negative index values, and wet periods are represented as positive index values. Absolute values greater than 3 indicate extreme wet or dry periods. The index incorporates antecedent precipitation, moisture supply, and moisture demand that may reflect the climate of previous years (Dai et al. 2004). Within the North Coast Drainage, recent (1980–2014) dry periods generally include 1980 to 1981, 1985 to 1994, 1999 to 2004, 2007 to 2009, and 2012 to 2014. Recent wet periods generally include 1982 to 1984, 1995 to 1998, 2005 to 2006, and 2010 to 2011. Of these, 1983, 1995, and 1998 were extremely wet, although no years were extremely dry (figure 5). From 1895 to 2014, the wettest year on record from 1895 to 2013 was 1983 (index value of 4.19) and the driest year on record was 2014 (index value of -2.73).

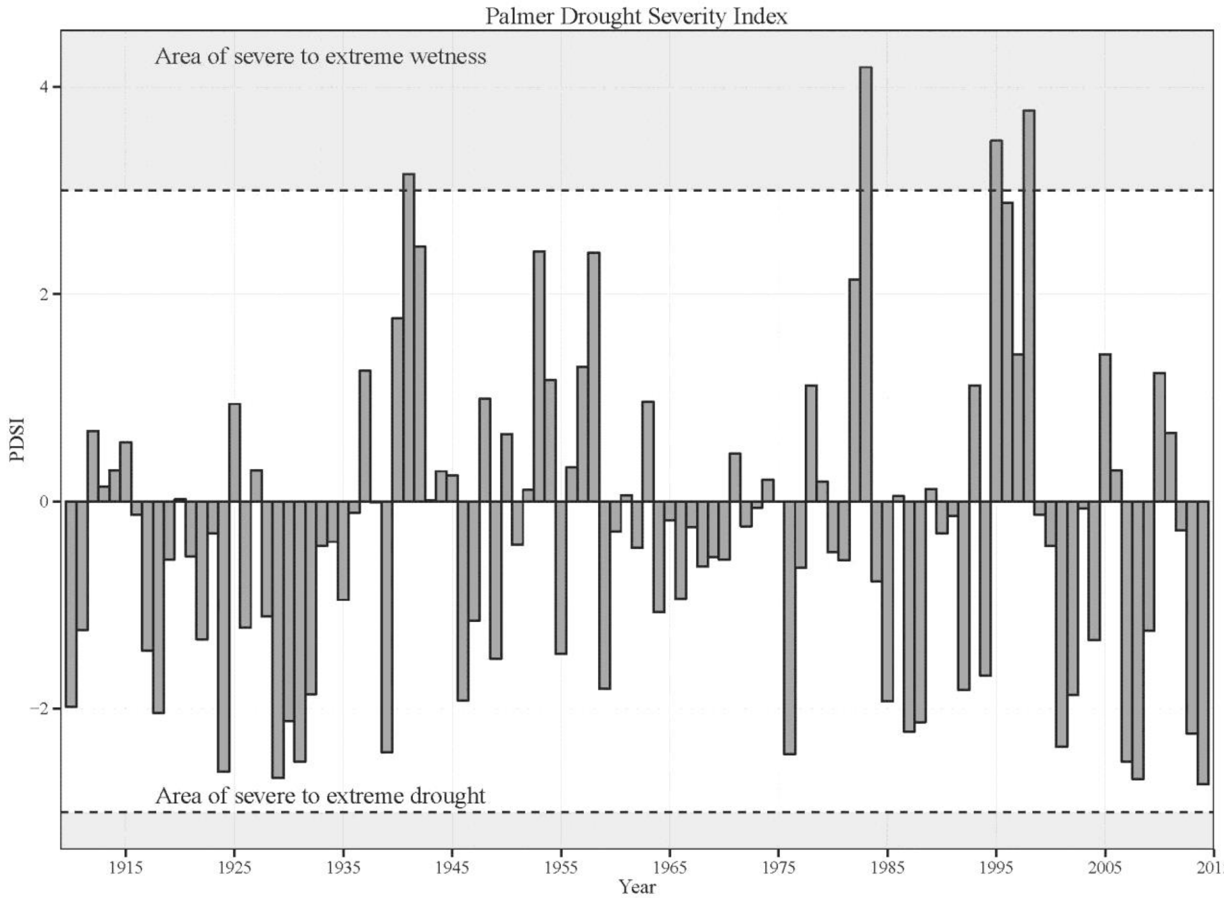

Figure 2. Palmer Drought Severity Index for the North Coast Drainage of California, 1895–2014

Recent Conditions

Monthly precipitation and temperature data, averaged for the Eureka Woodley Island climate station near HBNWR (USHCN station 42910), were compared with data from PRISM clipped to the Humboldt Bay drainage basin to show differences between local climate and climate that affects the RHI (figure 3 and 4). Precipitation was also compared with the Scotia climate station (CDEC Station SCA) to compare precipitation between HBWNR and inland areas which are representative of upstream conditions in the Humboldt Bay drainage basin. Temperature was not available at the Scotia climate station.

The mean monthly temperature near HBNWR ranged from 41.1 to 61.4 °F (based on data from 1985 to 2014) with minimum temperatures in January and December and maximum temperatures in August (figure 3), and is greater than temperatures averaged over the drainage basin. The mean monthly temperature averaged over the Humboldt Bay Drainage Basin ranged from 33.8 to 55.1 °F (based on data from 1984 to 2013) with timing similar to near the refuge (figure 4). Over the period 1985–2014, the greatest mean daily temperature near HBNWR occurred on July 8th, 1991 (72 °F). Over the same period, the

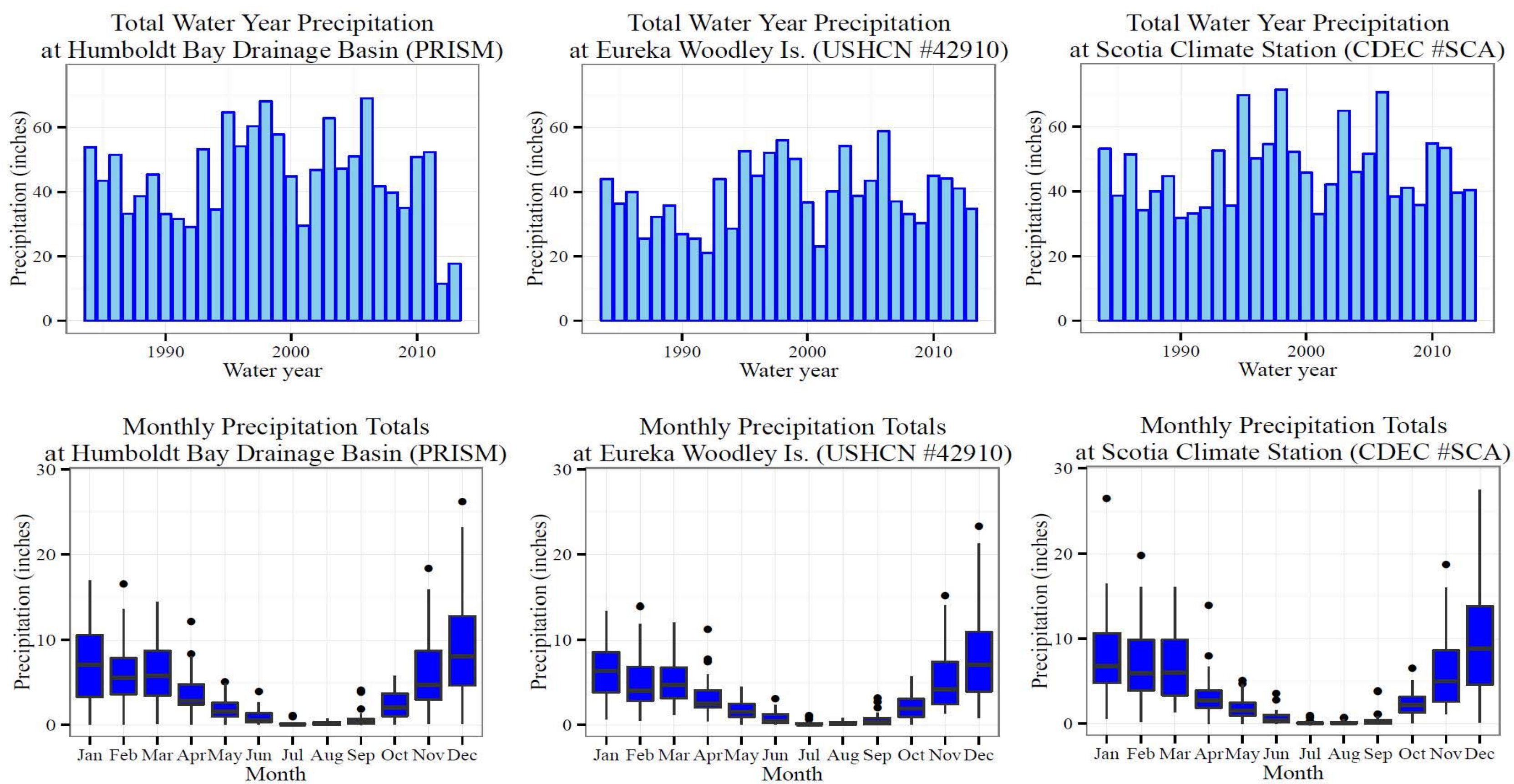

Figure 3. Monthly and annual precipitation for PRISM averaged over the Humboldt Bay drainage basin, Eureka Woodley Island climate station, and Scotia climate station 1985–2014. USHCN, United States Historical Climatology Network

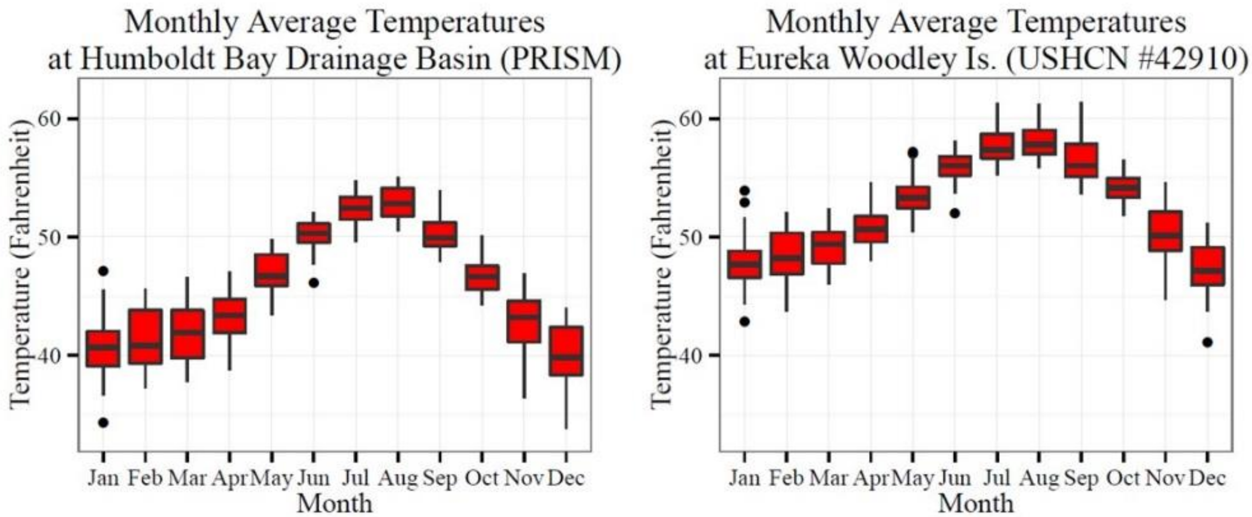

Figure 4. Monthly temperature for PRISM averaged over the Humboldt Bay drainage basin, Eureka Woodley Island climate station, 1985-2014. USHCN, United States Historical Climatology Network.

lowest mean daily temperature near HBNWR occurred on January 18th and February 22nd, 1995 (26 degrees). Near HBNWR, the maximum daily temperature has not gone above 87 degrees F and minimum daily temperature has not gone below 21 degrees F since 1985.

Precipitation varied somewhat between the Humboldt Bay Drainage Basin, Eureka Woodley Island climate station near HBNWR, and Scotia climate station farther inland. Precipitation was generally lowest near HBNWR with a mean total water year precipitation of 38.4 inches per year (ranging from 20.7 to 58.8 inches per year)[12] near the refuge. Precipitation was highest at the Scotia climate station farther inland, with a mean total water year precipitation of 45.7 inches per year (ranging from 18.3 to 71.5 inches per year[13]). Mean monthly total precipitation near HBNWR ranged from 0 to 23.3 inches per month, whereas the mean monthly precipitation at the Scotia climate station ranged from 0 to 27.4 inches per month. The greatest precipitation generally occurs in December. June–September is generally driest with the exception of some rare small rain events (figure 3).

[12] Data are from Eureka Woodley Island (USHCN station 42910) for water years 1985–2014.

[13] Data are from Scotia climate station (CDEC station SCA) for water years 1985–2014.

Over the period 1985–2014, the greatest precipitation near HBNWR[14] in 1 day was on December 27th, 2002 (6.79 inches), followed by December 8th, 1996 (4.86 inches).

Historic Climate Trends

One might expect a greater likelihood of warmer conditions near HBNWR during El Niño (negative phase of the SOI), warm phase of PDO, and positive phase Pacific North American pattern (PNA) (appendix A figure A1-A3; appendix B table B2-B4). Statistically significant differences in both maximum and minimum temperatures were observed at the Eureka Woodley Island climate station for the phases of PDO, PNA, and SOI. However, no significant associations between teleconnection index values and temperature were observed in the Humboldt Bay Drainage Basin. No statistically significant associations between teleconnections and precipitation were observed at any location.

Many seasons and months showed increases in maximum or minimum temperature near the refuge over the entire period of record (1910–2014) or from 1925 or 1950 to 2014 (figure 5). Most increasing trends were for maximum temperature. Only cool season maximum temperatures near HBNWR continued to show trends after 1985. Increases in cool season temperatures were relatively small and ranged from 0.01 to 0.05 °F per year (ranging from 1.3 to 2.4 °F over the time periods tested). Temperatures during all other months and seasons have stabilized.

Some decreases in annual and cool season precipitation were observed in the Humboldt Drainage Basin and at the Scotia climate station, but precipitation has generally stabilized since 1985 at all locations. Median decreases in annual precipitation at Humboldt Bay Drainage Basin and Scotia climate station were 10.1 and 10.6 inches respectively over the period 1950-2013 (.15 to .17 inches per year respectively); however, no trends were observed since 1985. Decreases in January and March precipitation were also observed for these locations in several time periods. Neglible increases in July precipitation were observed for Humboldt Drainage Basin and Scotia climate station from 1925 to current (ranging from .02 to .03 inches over the time period tested); July typically does not receive much precipitation.

[14] Data are from Eureka Woodley Island (USHCN station 42910)

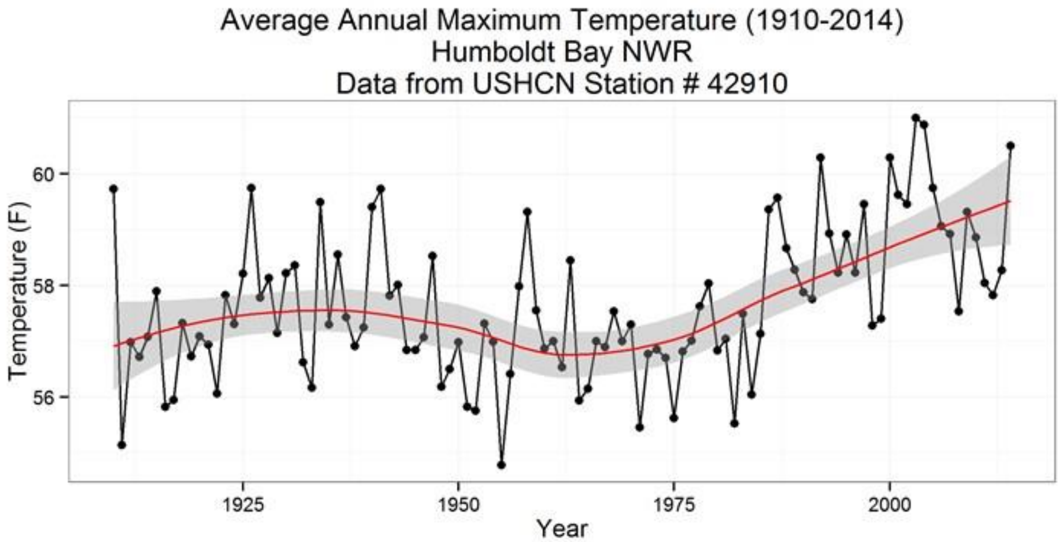

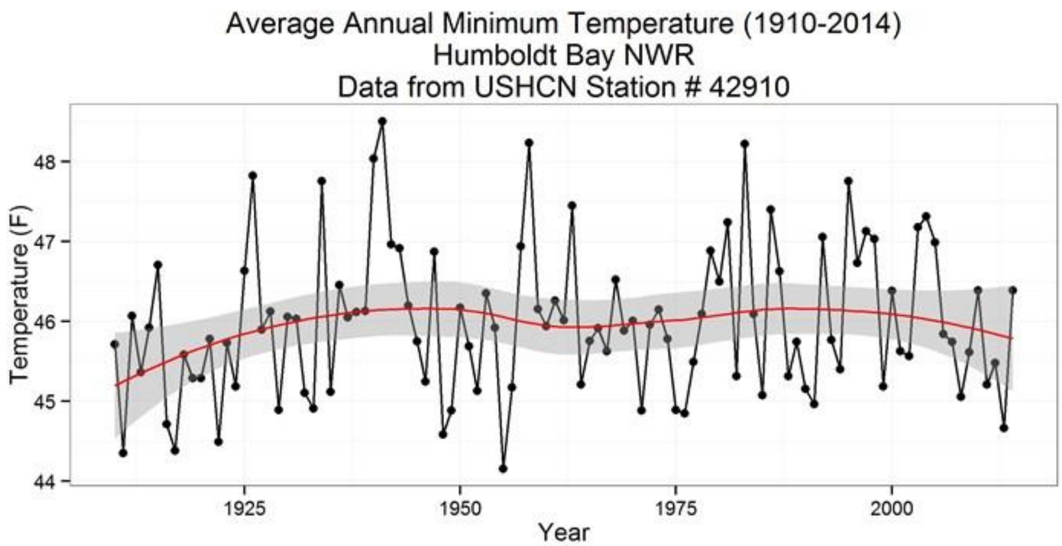

Figure 5. Trends in annual maximum and minimum temperature at Eureka Woodley Island climate station, 1910–2014

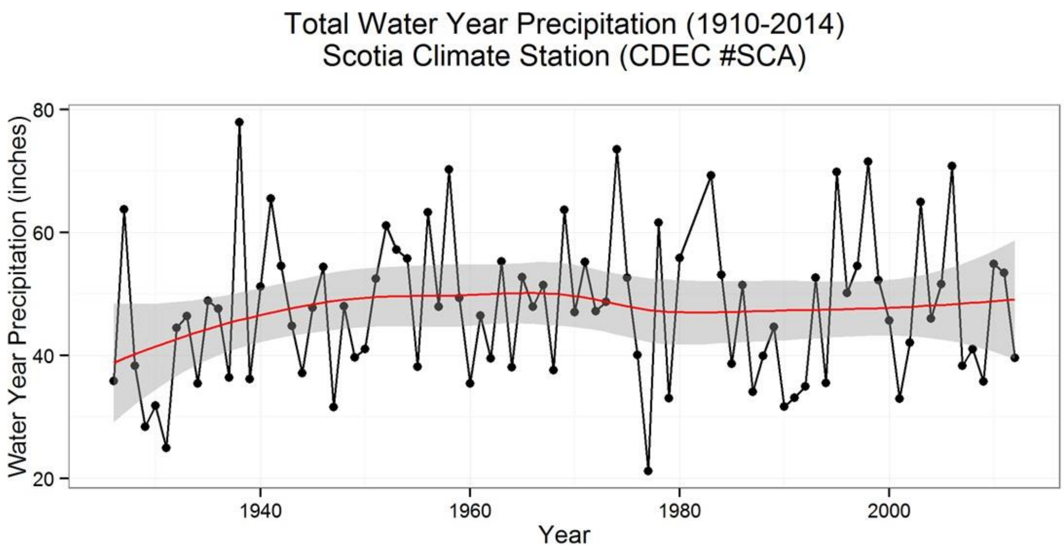

Figure 6. Trends in total annual precipitation at the Scotia climate station, 1925–2014

Climate Change

Temperature and Precipitation

Climate change could shift the hydroclimate of the western United States. The warming of 0.6–1.1 °F observed during the last half century over the western United States affected the relationship between climate and hydrologic response (Smith et al. 2000; Barnett et al. 2008).

Regional climate change models for the northwest of California predict warmer winter temperatures, earlier warming in the spring, and increased summer temperatures. However, many of the observed changes are less pronounced for coastal areas and more extreme inland and at higher elevations (Point Blue Conservation Science 2011).

Climate change models for Northwestern California predict increases in mean temperature and frequency of hot spells, decreases in the frequency of extreme cold days, and earlier start and extended duration of the growing season by 2100. Annual temperatures are predicted to increase 3.1–3.4 degrees F and diurnal temperature range will increase by 0.18 to 0.36 °F by 2070 for the Northwestern California Ecoregion (Stralberg et al 2009 cited in Point Blue Conservation Science 2011). The number of days in Northwestern California exceeding 90 degrees F is projected to increase 9.5 days per year (although temperatures have never exceeded 90 degrees F at the Eureka Woodley Island

Station) along with a 27-day per year increase in the frequency of extremely hot days. On average, the frost-free growing season is projected to start 25 days sooner and last approximately 38 days longer. The models show the number of extreme cold days decreasing by 37 days along with 45 fewer days below 32 degrees F (Bell et al 2004 cited in Point Blue Conservation Science 2011).

Climate change predictions for precipitation vary greatly among different models. Some models show slightly drier future climate relative to current conditions. Regional climate model predictions show a decrease in mean annual precipitation of 4–15 inches by 2070 in Northwestern California (Point Blue Conservation Science, 2011). However, in contrast other earlier models show slightly increases (3 percent) for the North Coast by 2100 (Snyder et al. 2004 and Snyder and Sloan 2005 cited in Point Blue Conservation Science, 2011), but a 10 to 20 percent decrease for Northern California over the same time period (Cayan et al. 2008).

Even with a doubling of carbon dioxide, there will be few significant changes in extreme precipitation events (greater than the 95th percentile) in the North Coast region (Bell et al. 2004, cited in Point Blue Conservation Science, 2011). The frequency of El Nino warm tropical events was projected to remain about the same as historical simulations, and modeled El Nino events continued to be related to anomalous precipitation patterns throughout California (Cayan et al. 2008).

A trend toward later streamflow timing was observed for non-snowmelt dominated streams (including those in the Northwestern California). The center of mass of annual flow was observed to shift 5 to 25 days later, which is a trend opposite for the Sierra Nevada because of the influence of earlier snowmelt on streamflow in that region (Stewart et al. 2005 cited in Point Blue Conservation Science 2011).

Within and near HBNWR, changes in 30-year forecasts for precipitation and recharge values were uncertain among models, showing either decreases or increases by 2100. Changes in mean 30-year precipitation at HBNWR and within the Humboldt Climate RHI ranged from -19.2 to +28.6 percent of historic values (-8 to 11.9 inches) to -17.9 to +31.5 percent (-9.8 to 17.3 inches) respectively, with the GFDL Model showing the greatest decrease and CSIRO showing the greatest increase (figure 7; table 1). Precipitation changes were very similar for HBNWR and the Climate RHI, although decreases were slightly greater and increases were slightly lesser for the Climate RHI (table 1). Changes in recharge had the greatest range in percent change from historical values, ranging from -27.19 to 48.6 percent (-2.2 to 3.9 inches).

Changes in 30-year forecasts for maximum and minimum temperature showed an increase under all model and emission scenarios through 2100 (table 1). By 2100, increases in maximum temperature ranged from 3.8 to 7.8 °F, while increases in the mean minimum temperature ranged from 4.1 to 7.1 °F. The GFDL model showed the greater increase and BCCR and PCM models showed the least increase. PET, which is directly related to temperature, also showed an increase ranging from 4.6 to 9.9 percent compared with historical values.

Changes in 30-year forecasts for water demand showed an increase under all model and emission scenarios from 2070 to 2100 (table 1, figure 7). By 2070–2100, CWD increases ranged from 7 to 8.1 inches per year, representing an 11.9 to 19 percent increase in water demand, or an additional 19.9 to 129.3 acre-feet per year of water input required over the refuge to maintain current or future habitats. GFDL showed the greatest increase and CSIRO showed the least increase. The impact of these increases is not known because the fresh water input required to maintain habitat units was not quantified as part of this summary.

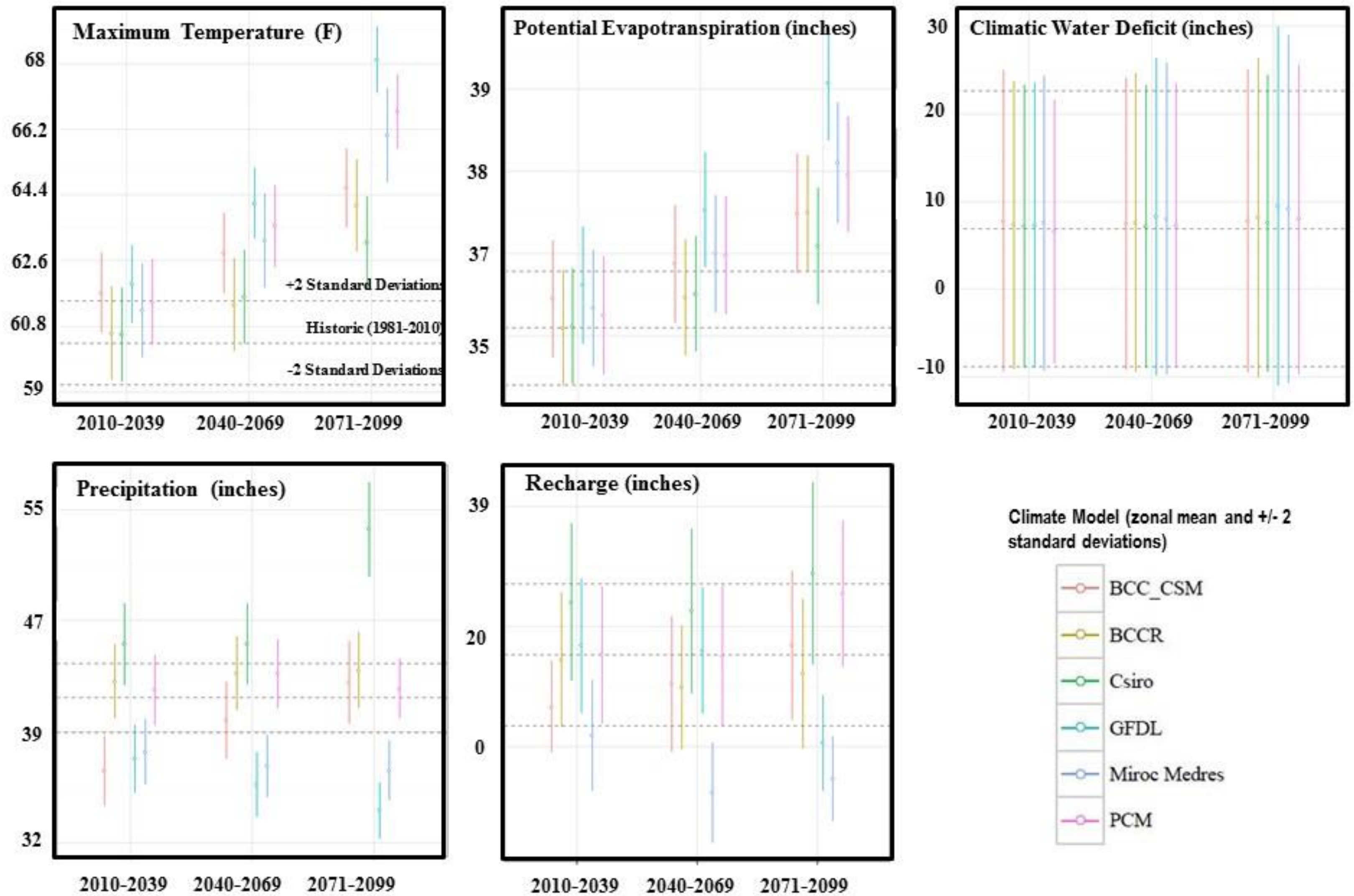

Figure 7. Historical and projected 30-year mean and spatial variability of potential evapotranspiration, maximum air temperature, climatic water deficit, and precipitation within the Humboldt Bay National Wildlife Refuge boundary, 1981–2100

Climate variable (inches or degrees Celcius)	*Bound-ary of considerat ion*	*1981-2010 Historic BCM*	*2010-2039 Csiro*	*2010-2039 BCCR*	*2010-2039 GFDL*	*2010-2039 Miroc Medres*	*2010-2039 BCC_CSM*	*2010-2039 PCM*	*2040-2069 Csiro*	*2040-2069 BCCR*	*2040-2069 GFDL*	*2040-2069 Miroc Medres*	*2040-2069 BCC_CSM*	*2040-2069 PCM*	*2070-2099 Csiro*	*2070-2099 BCCR*	*2070-2099 GFDL*	*2070-2099 Miroc Medres*	*2070-2099 BCC_CSM*	*2070-2099 PCM*
Precipitation (inches)	Refuge boundary	41.8	45.5	42.9	37.4	37.9	40.2	42.3	45.6	43.5	35.6	36.9	36.5	43.5	53.7	43.7	33.7	36.6	42.8	42.4
	Climate RHI	54.9	54.9	57.7	52.2	50.6	NA	56.3	61.3	58.4	48.7	49.3	53.7	57.3	72.2	58.8	45.1	49.0	57.2	55.2
Tmax (mean F)	Refuge boundary	60.3	60.6	60.6	61.9	61.2	61.7	61.5	61.6	61.4	64.2	63.1	62.8	63.5	63.1	64.1	68.1	66.0	64.6	66.7
Tmin (mean F)	Refuge boundary	46.1	47.1	47.0	47.8	47.7	47.9	46.7	48.1	47.9	49.7	49.4	49.0	48.2	50.0	50.4	53.2	52.0	50.6	50.2
Potential ET (inches)	Refuge boundary	35.6	35.6	35.5	36.2	35.8	36.0	35.7	36.0	36.0	37.2	36.6	36.5	36.6	36.7	37.2	39.1	37.9	37.2	37.7
Climatic Water Deficit (CWD, inches)	Refuge boundary	6.8	7.0	7.1	7.1	7.4	7.6	6.4	7.4	7.4	9.3	9.0	7.3	7.1	7.0	8.0	8.1	7.9	7.6	7.8
Recharge (inches)	Refuge boundary	8.1	9.5	8.5	6.8	7.0	6.7	8.2	9.4	8.6	6.3	6.7	7.5	8.5	12.0	8.9	5.8	6.8	8.6	8.2

Key: BCM, Basin Characterization Model (Flint and Flint, 2012); F = degrees Fahrenheit; ET = evapotranspiration

Csiro = Commonwealth Scientific and Industrial Organisation model; BCCR = Bergen Climate Model Version 2, ;

GFDL = General Circulation Model Climate Change Model from Geophysical Fluid Dynamics Laboratory);

Miroc Medres = Model for Interdiscipinary Research on Climate; BCC_CSM = Beijing Climate Center,

China Meterological Administration; PCM = General Circulation Model Climate Change Model from Parallel Climate Model

NA = not available

Notes: Csiro developed by the Centre for Australian Weather and Climate Research

BCCR developed by Bjerknes Centre for Climate Research (Norway)

Miroc Medres developed by the Center for Climate System Research, Tokyo, Japan and National Institute for Environmental Studies, Ibaraki, Japan

All climate variables were derived from 270 grid-cell data layers as input (precipitation and temperature) and output (snowpack, actual ET, potential ET, and CWD) from the Basin Characterization Model (BCM) (Flint and Flint, 2012; Flint and Flint, 2007) and clipped to the boundary of consideration

Historic snowpack was analyzed for the period 1971-2000

Table 1. Historic and future estimated values for selected climate variables for Humboldt Bay National Wildlife Refuge using the Basin Characterization Model

Sea- Level Rise

Global sea levels were estimated to have already risen 7.1 inches from 1900 to 2005 (Center for Ocean Solutions 2014). However, sea level rise is not uniform across California, as is evidenced by areas of the west coast which have shown moderate increases in sea level over the past several decades (California Energy Commission 2006, Largier et al. 2010).

Locally to Humboldt Bay, sea level rise is exacerbated by subsidence which results in rates of rise that are 2 to 3 times the rate of anywhere else in California. Subsidence is caused by the loss of sediment accretion from daily tidal inundation as a result of the diking and draining of salt marsh for agricultural and industrial use; former tidelands have compacted with decomposition of organic material (Pickart 2006 cited in Laird 2013). Rates of sea-level rise were measured to range from 0.1 to 0.23 inches per year within the various areas within and near HBNWR. Rates of subsidence were measured to range from -0.01 to – 0.14 inches per year (Patton et al 2014).

Estimates of global sea level rise for California suggest a possible sea level rise of 14.2 inches by 2050 and a high estimate of 55.1 inches by 2100 (Ramstorf 2007; Cayan et al. 2008). However, models and predictions vary geographically throughout the state. Due to climate change and tectonic plate movement, sea levels north of Cape Mendocino (12 miles south of the Humboldt Bay spit) are projected to change -1.6 (sea level fall) to +9 inches (sea level rise) by 2030, 12" by 2050, -1 to 18.9 inches by 2050, and 3.9 to 56.2 inches by 2100 (cited in Takekawa et al 2013).

Historic rates of sea level rise don't necessarily indicate observed rates in the future because sea level rise in the northern California coast and other areas are impacted by cyclic climate patterns. A combination of variables drives local variations in sea level including local wind and current patterns, salinity, changes in ocean temperatures, and large scale climate regimes such as the ENSO and PDO. ENSO and PDO both affect the weather, storms, and ocean temperature along the coast of California (Wingfield and Storlazzi 2007). ENSO events (shifting of the ENSO phase from La Niña to El Niño) are characterized by elevated water levels and waves caused by a southerly shift in the jet stream (Storlazzi and Wingfield 2005). El Nino events with elevated water temperatures have increased sea levels for several winter months by as much as 1 foot, as evidenced by the King Tide event at Humboldt Bay in 1983 (Laird, 2013). Studies by Bromirski et al. (2011) have indicated that the PDO could be driving climate changes that affect variability of sea levels. The PDO has caused large-scale shifts in the temperature pattern of the ocean. Cooler phases of PDO are associated with decreases in sea level rise, whereas warmer phases are associated with increases. The resultant variability of sea level along the California coast may exceed global average sea level at times (Bromirski et al. 2011).

HBNWR and nearby areas are vulnerable to sea level rise and overtopping of dikes and levees by waves as a result of storms, which could be compounded by seismic activity. Based upon existing conditions not including subsidence, a sea level rise of 12 inches plus an extreme high tide event would expose approximately 11 miles of dikes (28 percent) to overtopping in all hydrologic units of Humboldt Bay (Laird 2013). Because of the effect of subsidence, HBNWR could realize a relative sea level rise of 12 inches sooner than 2050 (Laird 2013). A large earthquake (greater than 8 on the Richter scale) would cause some coastal areas including Humboldt Bay to immediately subside and relative sea level to rise, which may result in relative sea-level rise of an additional 40 inches or more over projected levels (cited in Takekawa et al. 2013).

References

Bromirski, P.D.; Miller, A.J.; Flick, R.E.; Auad, G. 2011. Dynamical suppression of sea level rise along the Pacific coast of North America: Indications for imminent acceleration. Journal of Geophysical Research—Oceans. <http://onlinelibrary.wiley.com/doi/10.1029/2010JC006759/pdf> accessed January 2014.

California Department of Water Resources. 2015a. California Irrigation Management Information System (CIMIS) <http://wwwcimis.water.ca.gov/cimis/welcome.jsp> accessed April 2015.

California Department of Water Resources. 2015b. CDEC—California Data Exchange Center. <http://cdec.water.ca.gov/> accessed April 2015.

California Energy Commission. 2006. Our changing climate: assessing the risks to California. 16 p. <http://meteora.ucsd.edu/cap/pdffiles/CA_climate_Scenarios.pdf> accessed September 2014.

Cayan, D.; Bromirski, P.; Hayhoe, K.; Tyree, M.; Dettinger, M.; Flick, R. 2008. Climate change projections of sea level extremes along the California coast. Climatic Change, 87(0), 57-73. DOI 10.1007/s10584-007-9377-6. <http://meteora.ucsd.edu/cap/pdffiles/Cayan_sealevel_jan2008.pdf> accessed January 2014.

Cayan, D.R.; Dettinger, M.D.; Diaz, H.F.; Graham, N.E. 1998. Decadal variability of precipitation over western North America. Journal of Climatology 11:3148–3166.

Center for Ocean Solutions. 2014. Climate change and Monterey Bay: About sea level rise and impacts from sea level rise. <http://www.centerforoceansolutions.org/montereybay/about-sea level-rise-california#why> accessed May 2014.

Dai, A.; Trenbreth, K.E.; Qian, T. 2004. A global dataset of Palmer Drought Severity Index for 1870–2002: Relationship with soil moisture and effects on surface warming. Journal of Hydrometeorology 5:1117–1130. <http://www.cgd.ucar.edu/cas/adai/papers/Dai_pdsi_paper.pdf> accessed March 2013.

Dettinger, M.D.; Cayan, D.R.; Diaz, H.F.; Meko, D.M. 1998. North–south precipitation patterns in western North America on interannual-to-decadal timescales. Journal of Climatology 11:3,095–3,111.

Dietz, E.J. 1989. Teaching regression in a nonparametric statistics course. American Statistician 43:35–40.

Easterling, D.R.; Karl, T.R.; Lawrimore, J.H.; Del Greco, S.A. 1999. United States Historical Climatology Network daily temperature, precipitation, and snow data for 1871–1997. ORNL/CDIAC-118, NDP-070. Carbon Dioxide Information Analysis Center, Oak Ridge National Laboratory, U.S. Department of Energy, Oak Ridge, Tennessee. <http://cdiac.ornl.gov/epubs/ndp/ushcn/ushcn.html> accessed April 2015.

ESRI. 2012. Environmental Systems Research Institute ArcGIS 10.1: Iso Cluster Unsupervised Classification (Spatial Analyst). ArcGIS Help 10.1. <http://resources.arcgis.com/en/help/main/10.1/index.html#//009z000000pn000000> accessed April 2015.

Flint L.E.; Flint A.L.; Stolp B.J.; Danskin W.R. 2012. A basin-scale approach for assessing water resources in a semiarid environment: San Diego region. California and Mexico. Hydrology and Earth System Sciences 16:1–17.

Flint, A.L.; Flint, L.E. 2007. Application of the basin characterization model to estimate in-place recharge and runoff potential in the Basin and Range carbonate-rock aquifer system, White Pine County, Nevada, and adjacent areas in Nevada and Utah: U.S. Geological Survey Scientific Investigations Report 2007-5099. 20 p. <http://pubs.usgs.gov/sir/2007/5099/> accessed September 2014.

Francis, R.C.; Hare, S.R.; Hollowed, A.B.; Wooster, W.S. 1998. Effects of interdecadal climate variability on the oceanic ecosystems of the Northeast. Pacific Fisheries Oceanography 7:1–21.

Gershunov, A.; Barnett, T.P. 1998. Interdecadal modulation of ENSO teleconnections: Bulletin of the American Meteorological Society 79(12):2715–2725.

Griffith, G.E., Omernik, J.M., McGinley, M. 2008. Ecoregions of the United States-Level IV (EPA): The Encyclopedia of Earth. http://www.eoearth.org/article/Ecoregions_of_the_United_States-Level_IV_(EPA) accessed April 2015.

Helsel, D.R.; Hirsch, R.M. 2002. Statistical methods in water resources. New York: Elsevier. 522 p.

Kendall, M.; Gibbons, J.D. 1990. Rank correlation methods. 5th edition. New York: Oxford University Press. 260 p.

Laird, A. 2013. Humboldt Bay Shoreline Inventory, Mapping, and Sea Level Rise Vulnerability Assessment <http://www.humboldtbaykeeper.org/images/PDF/vulnerabilityrating.pdf>.

Largier, J.; Cheng, B.S.; Higgason, K.D. (eds.). 2010. Climate change impacts: Gulf of the Farallones and Cordell Bank National Marine Sanctuaries. <http://sanctuaries.noaa.gov/science/conservation/fb_cbnms_climate.html> accessed January 2014.

National Center for Atmospheric Research. 2013. Global climate change indicators. National Oceanic and Atmospheric Administration. <http://www.cgd.ucar.edu/cas/catalog/climind/pdsi.html> accessed February 2015.

National Oceanic and Atmospheric Administration. 2014b. El Niño theme page. <http://www.pmel.noaa.gov/tao/elnino/el-nino-story.html> accessed September 2014.

National Oceanic and Atmospheric Administration. 2014c. Southern Oscillation Index theme page. <http://www.ncdc.noaa.gov/teleconnections/enso/indicators/soi.php> accessed September 2014.

National Oceanic and Atmospheric Administration. 2014d. National Climatic Data Center. 2014d. Pacific Decadal Oscillation. <http://www.ncdc.noaa.gov/teleconnections/pdo/> accessed September 2014

National Oceanic and Atmospheric Administration. 2015a. Global Historical Climatology Network. <http://www.ncdc.noaa.gov/data-access/land-based-station-data/land-based-datasets/global-historical-climatology-network-ghcn> accessed April 2015.

National Oceanic and Atmospheric Administration. 2015b. El Niño theme page. <http://www.pmel.noaa.gov/tao/elnino/el-nino-story.html> accessed July 2015.

National Oceanic and Atmospheric Administration. 2015c. National Climatic Data Center. Pacific Decadal Oscillation. <http://www.ncdc.noaa.gov/teleconnections/pdo/> accessed July 2015.

National Oceanic and Atmospheric Administration. 2015d. National Climatic Data Center. Pacific/North American (PNA). <http://www.cpc.ncep.noaa.gov/data/teledoc/pna.shtml> accessed July 2015.

Nuss, Wendell. 2014. Climate and Meteorology of the Monterey Bay. Monterey Bay National Marine Sanctuary site characterization. <http://montereybay.noaa.gov/sitechar/clim1.html> accessed March. 2014.

Patton, J. R., T. B. Williams, J. Anderson, R. Burgette, and T. Leroy. 2014. Tectonic land level changes and their contribution to sea-level rise, Humboldt Bay region, Northern California.

Point Blue Conservation Science. 2011. Projected effects of climate change in California: Ecoregional summaries emphasizing consequences for wildlife. Version 1.0. <http://data.prbo.org/apps/bssc/uploads/Ecoregional021011.pdf.> accessed April 2014.

PRISM Climate Group. 2014. Normal annual precipitation grid for the conterminous United States. <http://prism.oregonstate.edu/> accessed August 2014.

Ramstorf, S. 2007. A semi-empirical approach to projecting future sea level rise. Science 13:1368–370. <http://www.pik-potsdam.de/~stefan/Publications/Nature/rahmstorf_science_2007.pdf> accessed January. 2014.

Redmond, K.T.; Koch, R.W. 1991. Surface climate and streamflow variability in the western United States and their relationship to large-scale circulation indices. Water Resources Research 27:2381–2399.

Richard, M.; Mustafa, B.; Sander, B.; Eduardo, C.; Tim, C.; Jae, E.; Ismail, E.; Seita, E.; Lin, E.; Kathy, H.; Roger, J.; Mikiko, K.; Jessica, K.; Jean, F.L.; Martin, M.; Ben, M.; Jerry, M.; Leo, M.; John, M.; Nebojsa, N.; Brian, O.; Ramon, P.; Keywan, R.; Steven, R.; Paul, R.; Ron, S.; Detlef, V.V.; John, W.; Tom, W.; Jean, P.V.Y.; Monika, Z. 2008. Towards new scenarios for analysis of emissions, climate change, impacts, and response strategies. Intergovernmental Panel on Climate Change. Geneva. 132 p. <http://www.aimes.ucar.edu/docs/IPCC.meetingreport.final.pdf> accessed February 2015.

Ruffner, J.A. 1985. Climates of the states: National Oceanic and Atmospheric Administration narrative summaries, tables, and maps for each state, with overview of state climatologist programs. 3rd ed. Detroit, Mich. Gale Research Company 1985. <http://www.wrcc.dri.edu/narratives/CALIFORNIA.htm> accessed April 2014.

Seaber, P.R., Kapinos, F.P., and Knapp, G.L., 1987, Hydrologic Unit Maps: U.S. Geological Survey Water-Supply Paper 2294, 63 p.

Sen, P.K. 1968. On a class of aligned rank order tests in two-way layouts. Annals of Mathematical Statistics 39:1115–1124.

Solomon, S.; Qin, D.; Manning, M.; Chen, Z.; Marquis M.; Averyt, K.B.; Tingor, M.; Miller, H.L. eds. 2007. Climate change 2007: The physical science basis. In: Contribution of the Working Group I to the fourth assessment report of the Intergovernmental Panel on Climate Change. Cambridge University Presswood.

Storlazzi, C.D.; Wingfield, D.K. 2005. The spatial and temporal variability in oceanographic and meteorologic forcing along central California. JUSGS Scientific Investigations Report 2005-5085. <http://pubs.usgs.gov/sir/2005/5085/> accessed January. 2014.

Takekawa, J.Y., Thorne, K.M., Buffington, K.J., Freeman, C.M., Powelson, K.W., and Block G. 2013. Assessing marsh response from sea-level rise applying local site conditions: Humboldt Bay National Wildlife Refuge. Unpubl. Data Summary Report. USGS Western Ecological Research Center, Vallejo, CA. 45pp + Appendices

The R Project for Statistical Computing. 2014. <http://www.r-project.org/> accessed September 2014.

U.S. Fish and Wildlife Service. 2005. Final comprehensive conservation plan of Humboldt Bay National Wildlife Refuge.

<http://www.fws.gov/refuge/humboldt_bay/what_we_do/conservation.html> accessed April 2015.

U.S. Geological Survey. 2015. National Hydrography Dataset (NHD). http://nhd.usgs.gov/ Accessed April 2015

University of California–Davis. 2014. Statewide integrated pest management program California weather database. <http://www.ipm.ucdavis.edu/WEATHER/about_weather.html> accessed April 2015.

University of Utah. 2015. MesoWest Climate Data Portal. University of Utah. <http://mesowest.utah.edu/index.html> accessed April 2015.

Western Regional Climate Center. 2008. Local Climate Data Summaries for Western U.S. (2008): Arcata. <http://www.wrcc.dri.edu/summary/acv.ca.html> Accessed April 2015.

Wingfield, D. K.; , & Storlazzi, C. D. 2007. Spatial and temporal variability in oceanographic and meteorologic forcing along Central California and its implications on nearshore processes. Journal of Marine Systems. v. 68. p.: 457-–472.

Glossary

Actual evapotranspiration (AET) - AET is the amount of water that evaporates from the surface and is transpired by plants if the total amount of water is not limited

Basin Characterization Model (BCM) - BCM is a water balance model that is driven by high resolution (270-meter) temperature and precipitation data downscaled from PRISM that is used to characterize water budget at the land surface.

Climatic Water Deficit (CWD) - CWD is the amount of water by which potential evapotranspiration (PET) exceeds actual evapotranspiration (AET), and can be thought of as the amount of additional water that would have evaporated or transpired had it been present in the soils given the AET. This calculation is an estimate of drought stress on soils and plants.

Cluster analysis - Cluster analysis or clustering is the task of grouping a set of objects in such a way that objects in the same group (called a cluster) are more similar (in some sense or another) to each other than to those in other groups (clusters).

El Niño–Southern Oscillation (ENSO) - ENSO is an oscillation of the ocean temperatures in the equatorial Pacific that has implications for global weather. El Niño is characterized by unusually warm ocean temperatures, whereas La Niña is characterized by unusually cool temperatures in the equatorial Pacific. The SOI is a measure of El Niño and is an index that combines the Southern Oscillation (differences in ocean temperatures in the equatorial Pacific), and is computed as monthly mean sea level pressure anomalies at the locations of Tahiti and Darwin islands.

General Circulation Model - A general circulation model (GCM), a type of climate model, is a mathematical model of the general circulation of a planetary atmosphere or ocean and based on the Navier–Stokes equations on a rotating sphere with thermodynamic terms for various energy sources (radiation, latent heat).

Groundwater Recharge - A hydrologic process where water moves downward from surface water to storage in groundwater.

Kendall's tau statistical time-series trend test - The Kendall's tau test is a non-parametric statistical test that can be used to indicate the likelihood of upward or downward trends in data with time.
Kruskal–Wallis test - The Kruskal-Wallis test is a non-parametric rank-based nonparametric test that can be used to determine if there are statistically significant differences between two or more groups of independent variables.

Maximum Likelihood Estimator - In statistics, maximum-likelihood estimation (MLE) is a method of estimating the parameters of a statistical model. When applied to a data set and given a statistical model, maximum-likelihood estimation provides estimates for the model's parameters. The method of maximum likelihood selects the set of values of the model parameters that maximizes the likelihood function. Intuitively, this maximizes the "agreement" of the selected model with the observed data.

Pacific Decadal Oscillation - The PDO is a global teleconnection pattern of Pacific climate variability that is measured as a standardized index of warm or cool surface waters in the Pacific Ocean north of 20 degrees latitude. This pattern shifts phases on an inter-decadal scale (20–30 years).
Pacific North American pattern - The PNA is one of the most recognized, influential climate patterns in the Northern Hemisphere mid-latitudes beyond the tropics. It consists of pressure anomalies in the geopotential height fields (typically at 700 or 500mb) observed over the western and eastern United States.

Palmer Drought Severity Index (PDSI) - The Palmer Drought Severity Index (PDSI) responds to long-term weather conditions and provides a coarse-level indication of regional meteorological wet or dry periods (National Center for Atmospheric Research 2013, figure 2). The index uses 0 as a normal, dry years are represented as negative index values, and wet periods are represented as positive index values. Absolute values greater than 3 indicate extreme wet or dry periods.

Parameter-elevation Regressions on Independent Slopes Model (PRISM) - PRISM is an analytical model that uses climate monitoring data, a digital elevation model (DEM; topography and orographic features), and atmospheric characteristics to generate estimates of monthly and annual precipitation and temperature.

Potential evapotranspiration (PET) - PET is the total amount of water that can evaporate from the ground surface or be transpired by plants.

Raster - A raster consists of a matrix of cells (or pixels) organized into rows and columns (or a grid) where each cell contains a value representing information, such as temperature. Rasters are digital aerial photographs, imagery from satellites, digital pictures, or even scanned maps.
Region of Hydrologic Influence - The purpose of an RHI is to represent an area of similar climate or hydrologic conditions as the refuge, and to select areas that likely have an influence on surface water conditions at a specific location.

Runoff - Surface runoff (also known as overland flow) is the flow of water that occurs when excess stormwater, meltwater, or other sources flows over the earth's surface.

Southern Oscillation Index (SOI) - The SOI is an index that combines the Southern Oscillation (differences in ocean temperatures in the equatorial Pacific) and is computed as monthly mean sea level pressure anomalies at the islands of Tahiti and Darwin.

Subsidence (climatic) - Areas where large masses of cooler, drier air descend from higher to lower elevations, causing an increase in barometric pressure

Subsidence (geologic) - The gradual or sudden caving or sinking of an area of land
Teleconnection indices - Teleconnection indices are used to measure patterns in teleconnections, which refer to recurring and persistent, large-scale patterns of pressure and circulation anomalies that span vast geographical areas.

Appendix A

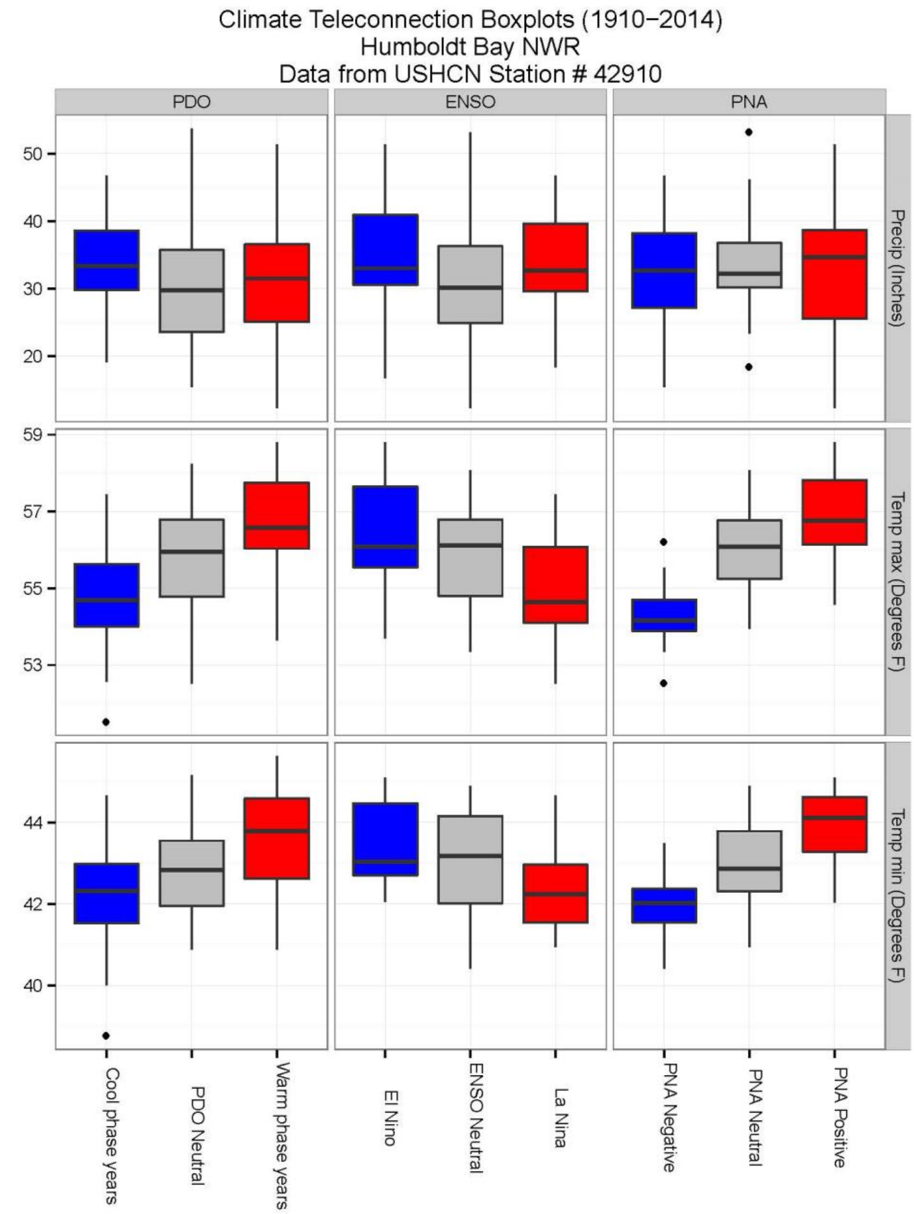

Figure A1. Comparison of mean October-March precipitation and temperature and July-November El Niño Southern Oscillation (SOI) for the previous year, near Humboldt Bay National Wildlife Refuge (Eureka Woodley Island Climate Station) for the period 1951–2010 (PDO, Pacific Decadal Oscillation; ENSO, El Niño Southern Oscillation; precipitation is in inches; temperature is in degrees Fahrenheit)

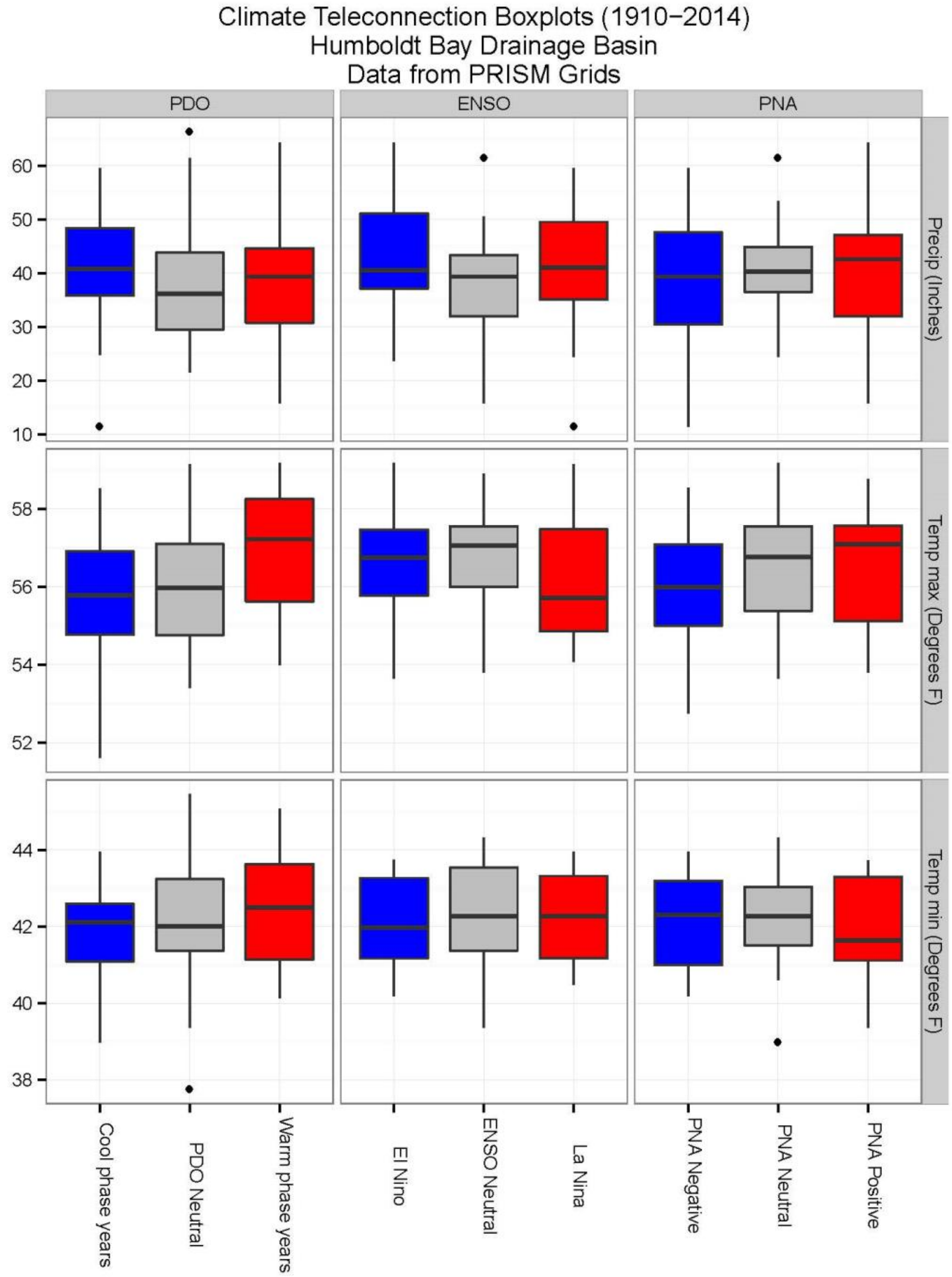

Figure A2. Comparison of mean October-March precipitation and temperature and July-November El Niño Southern Oscillation (SOI) for the previous year, near Humboldt Drainage Basin (PRISM) for the period 1951–2010 (PDO, Pacific Decadal Oscillation; ENSO, El Niño Southern Oscillation; precipitation is in inches; temperature is in degrees Fahrenheit)

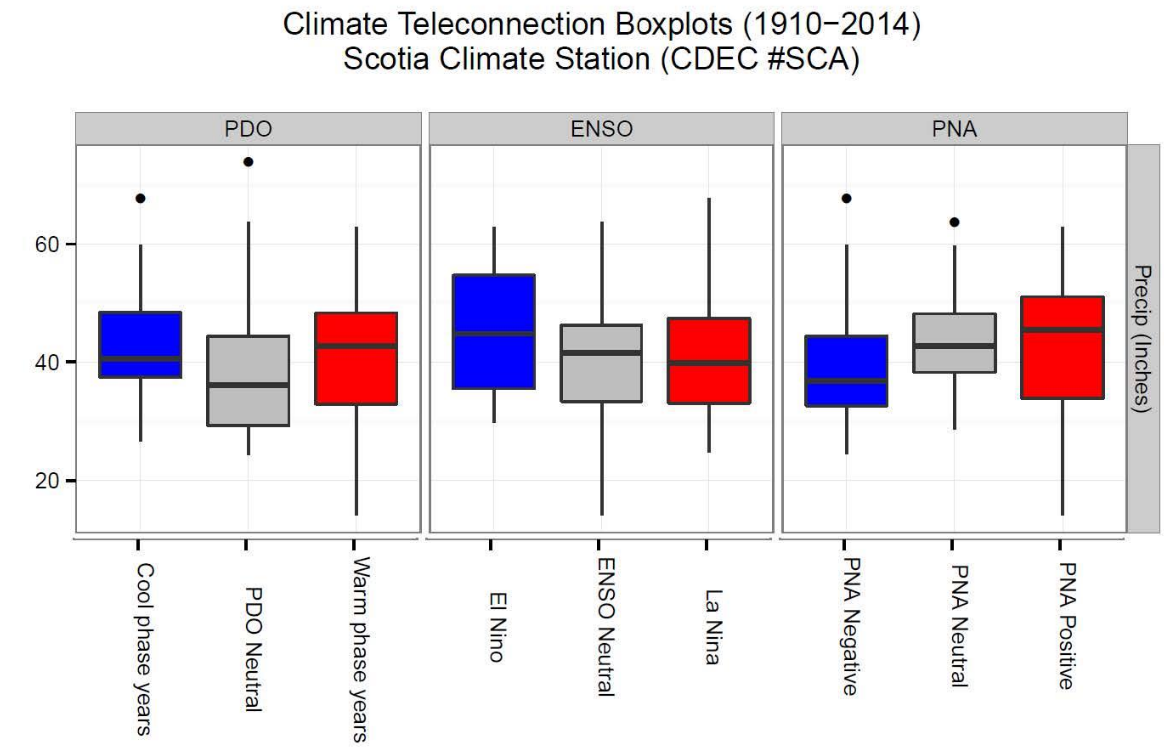

Figure A2. Comparison of mean October-March precipitation and July-November El Niño Southern Oscillation (SOI) for the previous year at the Scotia Climate Station for the period 1951–2010 (PDO, Pacific Decadal Oscillation; ENSO, El Niño Southern Oscillation; precipitation is in inches)

Appendix B

Table B1. Climate stations on and near Humboldt Bay National Wildlife Refuge.

Map Number (figure 7)	*Station Name*	*Station Operator*	*Agency/network hosting data server*	*Station Identification*	*Period of Record*	*Temporal resolution - Temp*	*Temporal resolution - Evap*	*Temporal resolution - Precip*	*Temporal resolution - Humidity*	*Temporal resolution - Sol. Rad.*	*Temporal resolution - Wind Speed*	*Eleva-tion (feet)*
1	Van Duzen R Nr Bridgeville At Grizzly Creek*	USGS and CADWR	CADWR	BRI	1984-1997			D				358
2	Scotia	NWS	CADWR	SCA	1925-present			M				139
3	Fortuna Rohnervill	NWS	UOU	KFOT	2011-present	H		H	H		H	377
4	Cw5061 Fortuna	IO	UOU	C5061	2006-present	H		H	H	H	H	197
5	K6Pij Fortuna	IO	UOU	AT493	2010-present	H		H	H		H	196
6	Fortuna 0.9 Ssw, Ca Us*	NCDC	NCDC	GHCND:US1CAHM0011	2008-2010			D				12
7	Fortuna 0.9 Ssw, Ca Us*	NCDC	NCDC	GHCND:US1CAHM0011	2008-2010			D				11.9
8	Fortuna 1.3 S, Ca Us*	NCDC	NCDC	GHCND:US1CAHM0020	2009-present			D				11.9
9	Fortuna 0.1 Nw, Ca Us	NCDC	NCDC	GHCND:US1CAHM0029	2010-present			D				6
10	Ferndale 2 Nw, Ca Us*	NCDC	NCDC	GHCND:USC00043030	1963-1973	D	D	D			D	0.9
11	Fortuna 1.5 Nw, Ca Us	NCDC	NCDC	GHCND:US1CAHM0012	2008-present	D						18.1
12	Ew4887 Fortuna	IO	UOU	E4877	2014-present	H		H	H		H	361
13	Hydesville 11.4 Ne, Ca Us	NCDC	NCDC	GHCND:US1CAHM0047	2013-present			D				227.2
14	Kneeland 2, Ca Us*	NCDC	NCDC	GHCND:USC00044586	1948-1951			D				247.2
15	Kneeland 3.5 Sse, Ca Us	NCDC	NCDC	GHCND:US1CAHM0052	2014-present			D				195.9
16	Dw0866 Eureka	IO	UOU	D0866	2008-present	H		H	H	H	H	79
17	Bayview 0.8 Se, Ca Us	NCDC	NCDC	GHCND:US1CAHM0016	2009-present			D				16.3
18	Eureka 3.0 Ssw, Ca Us	NCDC	NCDC	GHCND:US1CAHM0041	2011-present			D				9.3
19	Eureka 2.2 S, Ca Us	NCDC	NCDC	GHCND:US1CAHM0035	2010-present			D				18
20	Kneeland 0.4 Nnw, Ca Us	NCDC	NCDC	GHCND:US1CAHM0038	2011-present			D				186.5
21	Cw7137 Eureka	IO	UOU	C7137	2007-present	H		H	H	H	H	141
22	Butler Valley Ranch, Ca Us*	NCDC	NCDC	GHCND:USC00041233	1970-1975	D	D	D				39
23	North Spit	NWS	UOU	HBYC1	2008-present	H		H	H	H	H	0
24	Eureka 0.5 Sse, Ca Us*	NCDC	NCDC	GHCND:US1CAHM0018	2009-2010			D				10.7
25	Kneeland 4.8 Wnw, Ca Us	NCDC	NCDC	GHCND:US1CAHM0034	2010-present			D				9.8
26	Eureka 1.2 E, Ca Us	NCDC	NCDC	GHCND:US1CAHM0050	2014-present			D				6.4
27	Maple Creek	CALFIRE	CADWR	MPC	1995-present			M				370
28	Maple Creek California, Ca Us*	NCDC	NCDC	GHCND:USR0000CMAP	1995-2006	D						156.1
29	Eureka 0.4 Nw, Ca Us*	NCDC	NCDC	GHCND:US1CAHM0024	2009-2012			D				5.7
30	Eureka Woodley Island	NWS	CADWR	ERK	1905-present			D				20
31	Eureka Wso Woodley Island	NWS	UCDIPM	2910	1951-present	D		D				20
32	Eureka Weather Forecast Office Woodley Island, Ca	NCDC	NCDC	GHCND:USW00024213	1941-present	D		D			D	6.1
33	Eureka Wfo Woodley Is, Ca	NWS	USHCN	042910	1878-present	D		D				20
34	Dw2246 Eureka	IO	UOU	D2246	2009-present	H		H	H		H	18
35	Bayside 1.8 Se, Ca Us*	NCDC	NCDC	GHCND:US1CAHM0002	2008-2015			D				7.2
36	Korbel, Ca Us*	NCDC	NCDC	GHCND:US1CAHM0034	1959-1974			D				0
37	Arcata 1.0 Nw, Ca Us*	NCDC	NCDC	GHCND:US1CAHM0025	2009-2012			D				1.4
38	Dw8223 Arcata	IO	UOU	D8223	2011-present	H		H	H	H	H	184
39	Arcata 1.1 Nw, Ca Us*	NCDC	NCDC	GHCND:US1CAHM0019	2009-2011			D				1.6
40	Arcata 1.1 Ne, Ca Us	NCDC	NCDC	GHCND:US1CAHM0001	2008-present			D				39
41	Arcata 1.4 Nne, Ca Us	NCDC	NCDC	GHCND:US1CAHM0021	2009-present			D				26.9
42	Blue Lake 0.6 Nnw, Ca Us	NCDC	NCDC	GHCND:US1CAHM0039	2011-present			D				16.6
43	Arcata 2.1 Nnw, Ca Us	NCDC	NCDC	GHCND:US1CAHM0033	2010-present			D				3
44	Mckinleyville 7.3 Ese, Ca Us	NCDC	NCDC	GHCND:US1CAHM0005	2008-present			D				34
45	Mad River Near Arcata Ca	USGS and CADWR	CADWR	ARC	1999-present	H						33
46	Mckinleyville 2.7 Se, Ca Us	NCDC	NCDC	GHCND:US1CAHM0009	2008-present			D				30.2
47	Mckinleyville 1.2 Ssw, Ca Us*	NCDC	NCDC	GHCND:US1CAHM0040	2011-2014			D				5.4
48	Mckinleyville 0.7 Ese, Ca Us*	NCDC	NCDC	GHCND:US1CAHM0042	2011-2014			D				11.8
49	Mckinleyville 4.3 E, Ca Us	NCDC	NCDC	GHCND:US1CAHM0037	2011-present			D				16.1
50	Mckinleyville 2.1 Ne, Ca Us	NCDC	NCDC	GHCND:US1CAHM0051	2014-present			D				25.1
51	Mckinleyville 2.3 Ne, Ca Us	NCDC	NCDC	GHCND:US1CAHM0009	2008-present			D				25.1
52	Arcata Eureka Airport, Ca Us	NCDC	NCDC	GHCND:USW00024283	1992-present	D		D			D	18.6
53	Arcata Eureka Airport, Ca Us*	NCDC	NCDC	GHCND:USW00024245	1945-1946	D		D				18.6
54	Arcata Airport	NWS	UOU	KCAV	1997-present	H		H	H	H	H	217
55	Trinidad 4.2 Se, Ca Us*	NCDC	NCDC	GHCND:US1CAHM0027	2009-2010			D				1.7

Key: USGS = U.S. Geological Survey; CADWR = California Department of Water Resources; UCD = University of California Davis; IPM = Integrated Pest Management Database; USHCN = U.S. Historical Climatology Network; UOU = University of Utah

Temp = temperature; Evap = reference evapotranspiration; Sol. Rad. = Solar Radiation

H = hourly continuous; D = daily continuous; M = monthly continuous

* = Inactive site

Notes: Temporal resolution represents finest temporal resolution of parameter information available in digital form.

Table B2. Results of time-series trend analysis of annual and seasonal precipitation and temperature from the Eureka Woodley Island climate station (station 42910) near Humboldt Bay National Wildlife Refuge.

Time Period/Parameters	*1910-2014 tau*	*1910-2014 p-value*	*1910-2014 Percent of median*	*1910-2014 Median*	*1925-2014 tau*	*1925-2014 p-value*	*1925-2014 Percent of median*	*1925-2014 Median*	*1950-2014 tau*	*1950-2014 p-value*	*1950-2014 Percent of median*	*1950-2014 Median*	*1985-2014 tau*	*1985-2014 p-value*	*1985-2014 Percent of median*	*1985-2014 Median*
Annual																
Precipitation	0.11	0.11	0.13	37.03	0.07	0.36	0.10	37.19	-0.08	0.33	-0.16	38.81	0.19	0.145	0.88	36.77
Max Temperature	0.25	0.00	0.03	57.40	0.22	0.00	0.03	57.54	0.47	0.00	0.08	57.53	0.07	0.568	0.02	58.91
Average Temperature	0.22	0.00	0.02	51.65	0.15	0.04	0.02	51.78	0.33	0.00	0.05	51.67	0.04	0.777	0.01	52.46
Min Temperature	0.08	0.22	0.01	45.92	-0.04	0.59	0.00	46.01	-0.01	0.95	0.00	45.93	-0.08	0.556	-0.02	45.75
Winter																
Precipitation	0.05	0.48	0.09	17.58	0.05	0.51	0.10	17.75	-0.06	0.49	-0.17	18.28	-0.03	0.838	-0.23	18.59
Max Temperature	0.11	0.09	0.02	54.05	0.05	0.50	0.01	54.40	0.22	0.01	0.06	54.02	0.06	0.634	0.03	55.17
Average Temperature	0.08	0.25	0.02	47.53	-0.01	0.90	0.00	47.87	0.09	0.28	0.03	47.56	-0.01	0.973	-0.01	48.28
Min Temperature	0.03	0.69	0.01	41.18	-0.06	0.37	-0.02	41.43	-0.06	0.45	-0.02	41.23	-0.04	0.747	-0.02	41.20
Spring																
Precipitation	0.12	0.08	0.25	8.47	0.06	0.37	0.14	9.29	0.07	0.39	0.23	8.30	0.13	0.338	0.96	9.04
Max Temperature	0.19	0.00	0.03	55.67	0.16	0.02	0.03	55.82	0.44	0.00	0.11	55.70	-0.07	0.620	-0.03	57.40
Average Temperature	0.13	0.04	0.02	50.03	0.09	0.21	0.02	50.21	0.35	0.00	0.08	50.10	-0.14	0.269	-0.07	50.93
Min Temperature	0.02	0.76	0.00	44.50	-0.05	0.50	-0.01	44.57	0.14	0.11	0.04	44.50	-0.23	0.074	-0.13	44.85
Summer																
Precipitation	0.07	0.28	0.27	0.76	0.08	0.27	0.34	0.76	0.02	0.78	0.13	0.79	-0.04	0.775	-0.23	0.77
Max Temperature	0.33	0.00	0.05	60.60	0.34	0.00	0.06	60.80	0.54	0.00	0.13	60.83	0.15	0.239	0.06	62.65
Average Temperature	0.34	0.00	0.04	55.88	0.33	0.00	0.04	56.06	0.51	0.00	0.09	56.20	0.21	0.108	0.07	57.12
Min Temperature	0.27	0.00	0.02	51.10	0.20	0.01	0.02	51.13	0.33	0.00	0.05	51.13	0.19	0.138	0.05	51.73
Fall																
Precipitation	0.04	0.55	0.09	8.09	-0.01	0.91	-0.02	8.23	-0.14	0.11	-0.53	8.47	0.15	0.241	1.12	7.98
Max Temperature	0.13	0.05	0.01	59.70	0.14	0.05	0.02	59.63	0.20	0.02	0.04	59.70	0.17	0.192	0.06	60.43
Average Temperature	0.08	0.24	0.01	53.45	0.04	0.60	0.01	53.46	0.01	0.87	0.00	53.63	0.05	0.695	0.02	53.73
Min Temperature	-0.02	0.72	0.00	47.10	-0.12	0.09	-0.02	47.13	-0.24	0.00	-0.04	47.13	-0.05	0.721	-0.01	46.87
Cool Season																
Precipitation	0.09	0.17	0.17	15.58	0.04	0.58	0.09	16.11	-0.06	0.49	-0.16	16.62	0.08	0.547	0.70	15.37
Max Temperature	0.22	0.00	0.02	59.27	0.22	0.00	0.03	59.38	0.39	0.00	0.06	59.38	0.27	0.037	0.08	60.43
Average Temperature	0.19	0.00	0.02	53.50	0.14	0.05	0.01	53.59	0.21	0.01	0.03	53.63	0.12	0.353	0.04	54.04
Min Temperature	0.10	0.15	0.01	47.73	-0.01	0.94	0.00	47.84	-0.08	0.38	-0.01	47.88	0.03	0.844	0.02	47.82
January																
Precipitation	-0.03	0.64	-0.07	5.92	0.01	0.92	0.02	5.83	-0.17	0.04	-0.82	6.38	-0.08	0.571	-0.82	6.34
Max Temperature	0.13	0.05	0.04	54.00	0.10	0.15	0.03	53.95	0.26	0.00	0.11	53.90	0.04	0.734	0.04	55.05
Average Temperature	0.09	0.17	0.03	46.90	0.07	0.35	0.02	46.95	0.17	0.04	0.07	46.85	-0.03	0.830	-0.03	47.73
Min Temperature	0.04	0.59	0.01	40.50	0.01	0.88	0.00	40.50	0.04	0.61	0.02	40.50	-0.04	0.761	-0.04	40.60
February																
Precipitation	-0.01	0.90	-0.02	5.09	0.00	0.95	0.01	4.84	-0.03	0.73	-0.14	4.67	0.01	0.972	0.06	4.02
Max Temperature	0.13	0.06	0.03	54.10	0.06	0.38	0.02	54.15	0.16	0.06	0.06	54.10	-0.03	0.844	-0.02	55.70
Average Temperature	0.10	0.13	0.03	47.80	0.03	0.63	0.01	47.90	0.09	0.29	0.04	47.80	-0.07	0.605	-0.06	48.25
Min Temperature	0.06	0.41	0.02	41.30	-0.02	0.83	-0.01	41.60	-0.01	0.88	0.00	41.30	-0.06	0.655	-0.07	40.60
March																
Precipitation	0.15	0.03	0.40	4.70	0.10	0.18	0.29	4.72	0.03	0.73	0.12	4.91	0.12	0.353	1.12	4.82
Max Temperature	0.12	0.07	0.02	54.60	0.10	0.16	0.02	54.75	0.32	0.00	0.10	54.70	-0.12	0.353	-0.08	56.10
Average Temperature	0.08	0.21	0.02	48.40	0.05	0.47	0.01	48.50	0.24	0.00	0.08	48.40	-0.10	0.422	-0.07	49.23
Min Temperature	0.02	0.74	0.01	41.90	-0.01	0.85	0.00	42.05	0.11	0.19	0.05	41.90	-0.11	0.412	-0.12	42.05

Time Period/Parameters	*1910-2014 tau*	*1910-2014 p-value*	*1910-2014 Percent of median*	*1910-2014 Median*	*1925-2014 tau*	*1925-2014 p-value*	*1925-2014 Percent of median*	*1925-2014 Median*	*1950-2014 tau*	*1950-2014 p-value*	*1950-2014 Percent of median*	*1950-2014 Median*	*1985-2014 tau*	*1985-2014 p-value*	*1985-2014 Percent of median*	*1985-2014 Median*
April																
Precipitation	0.04	0.55	0.13	2.61	0.04	0.58	0.16	2.58	0.10	0.25	0.50	2.62	0.22	0.087	2.02	2.44
Max Temperature	0.12	0.08	0.02	55.50	0.14	0.05	0.03	55.45	0.43	0.00	0.10	55.30	-0.05	0.694	-0.03	56.75
Average Temperature	0.05	0.43	0.01	49.65	0.04	0.58	0.01	49.68	0.29	0.00	0.07	49.55	-0.18	0.164	-0.09	50.63
Min Temperature	-0.04	0.56	-0.01	44.10	-0.09	0.23	-0.02	44.25	0.10	0.23	0.02	43.90	-0.34	0.008	-0.16	44.65
May																
Precipitation	0.01	0.85	0.05	1.38	-0.03	0.72	-0.10	1.38	0.01	0.90	0.06	1.30	-0.14	0.287	-2.29	1.41
Max Temperature	0.23	0.00	0.04	57.30	0.19	0.01	0.04	57.60	0.37	0.00	0.12	57.60	-0.01	0.957	0.00	59.45
Average Temperature	0.17	0.01	0.03	52.10	0.13	0.07	0.03	52.30	0.33	0.00	0.08	52.25	-0.01	0.915	0.00	53.15
Min Temperature	0.02	0.72	0.00	47.00	-0.05	0.52	-0.01	47.05	0.12	0.15	0.03	46.70	-0.09	0.508	-0.05	47.50
June																
Precipitation	0.03	0.69	0.11	0.35	0.02	0.74	0.11	0.35	0.05	0.59	0.32	0.35	0.05	0.721	0.47	0.39
Max Temperature	0.22	0.00	0.04	59.60	0.21	0.00	0.05	59.65	0.44	0.00	0.14	59.60	0.18	0.163	0.08	62.20
Average Temperature	0.23	0.00	0.04	54.85	0.19	0.01	0.03	54.98	0.39	0.00	0.10	54.90	0.18	0.159	0.07	56.13
Min Temperature	0.14	0.04	0.02	49.80	0.04	0.55	0.01	49.90	0.21	0.01	0.04	49.80	0.11	0.381	0.05	50.30
July																
Precipitation	0.12	0.07	0.53	0.05	0.12	0.10	0.63	0.06	0.09	0.28	0.60	0.06	-0.20	0.136	-3.57	0.06
Max Temperature	0.32	0.00	0.05	60.60	0.32	0.00	0.06	60.60	0.51	0.00	0.13	60.70	0.06	0.655	0.04	62.95
Average Temperature	0.29	0.00	0.04	56.05	0.29	0.00	0.05	56.08	0.45	0.00	0.10	56.15	0.08	0.544	0.03	57.43
Min Temperature	0.19	0.00	0.03	51.40	0.17	0.02	0.03	51.50	0.26	0.00	0.06	51.60	0.06	0.642	0.04	52.05
August																
Precipitation	0.12	0.07	0.58	0.06	0.11	0.12	0.51	0.07	0.01	0.87	0.00	0.07	-0.03	0.844	0.00	0.08
Max Temperature	0.35	0.00	0.05	61.60	0.39	0.00	0.07	61.75	0.47	0.00	0.12	62.00	0.21	0.112	0.09	63.20
Average Temperature	0.33	0.00	0.04	56.80	0.33	0.00	0.05	56.93	0.36	0.00	0.08	57.15	0.18	0.158	0.08	58.10
Min Temperature	0.22	0.00	0.03	52.10	0.20	0.00	0.03	52.30	0.20	0.02	0.05	52.40	0.13	0.308	0.06	52.80
September																
Precipitation	-0.04	0.56	-0.17	0.55	-0.01	0.89	-0.03	0.57	-0.07	0.40	-0.51	0.60	0.12	0.353	1.66	0.35
Max Temperature	0.16	0.02	0.03	61.60	0.21	0.00	0.04	61.60	0.25	0.00	0.07	61.80	0.23	0.080	0.16	62.75
Average Temperature	0.14	0.03	0.02	55.90	0.14	0.05	0.02	55.90	0.14	0.11	0.04	55.95	0.18	0.175	0.10	56.38
Min Temperature	0.05	0.44	0.01	50.10	-0.01	0.91	0.00	50.25	-0.07	0.39	-0.02	50.30	0.05	0.721	0.02	50.00
October																
Precipitation	0.03	0.70	0.10	2.11	-0.05	0.44	-0.24	2.24	-0.10	0.24	-0.66	2.11	0.11	0.392	1.66	1.86
Max Temperature	0.17	0.01	0.02	60.20	0.17	0.02	0.03	60.15	0.20	0.02	0.05	60.40	0.22	0.086	0.10	60.90
Average Temperature	0.10	0.14	0.01	53.80	0.07	0.36	0.01	53.78	0.05	0.54	0.01	53.90	0.14	0.268	0.06	54.05
Min Temperature	0.00	0.98	0.00	47.50	-0.09	0.21	-0.02	47.50	-0.14	0.11	-0.04	47.30	-0.06	0.629	-0.03	46.95
November																
Precipitation	0.01	0.86	0.04	4.70	0.02	0.81	0.09	4.48	-0.09	0.29	-0.50	4.72	0.09	0.524	0.86	3.98
Max Temperature	-0.04	0.59	-0.01	57.30	-0.05	0.50	-0.01	57.30	0.03	0.77	0.01	57.30	-0.01	0.957	0.00	57.50
Average Temperature	-0.06	0.38	-0.01	50.70	-0.09	0.23	-0.02	50.70	-0.12	0.16	-0.04	50.65	-0.05	0.681	-0.03	50.15
Min Temperature	-0.05	0.42	-0.01	43.80	-0.11	0.14	-0.04	43.80	-0.22	0.01	-0.09	43.80	-0.08	0.544	-0.09	43.25
December																
Precipitation	0.09	0.16	0.29	6.11	0.06	0.39	0.20	6.44	0.05	0.55	0.24	6.52	0.11	0.392	1.16	7.05
Max Temperature	-0.02	0.74	0.00	54.50	-0.09	0.23	-0.02	54.65	0.05	0.59	0.01	54.20	0.03	0.830	0.02	54.85
Average Temperature	-0.05	0.44	-0.01	47.80	-0.12	0.08	-0.04	47.85	-0.08	0.34	-0.03	47.65	-0.02	0.886	-0.02	47.13
Min Temperature	-0.06	0.37	-0.02	41.20	-0.14	0.05	-0.05	41.25	-0.19	0.03	-0.10	41.10	-0.08	0.520	-0.05	39.95

Key: p-Value = probability level; tau = Kendall's tau

Notes: Precipitation is measured in inches, temperature is measured in degrees Fahrenheit

Results shaded in blue are statistically significant wetter/cooler trends (upward trends in precipitation and downward trends in temperature) at a p-value of 0.05

Results shaded in red are statistically significant warmer/drier trends (downward trends in precipitation and upward trends in temperature) at a p-value of 0.05

Table B3. Results of time-series trend analysis of annual and seasonal precipitation and temperature in the Humboldt Bay Drainage Basin near Humboldt Bay National Wildlife Refuge, calculated from PRISM averages.

Time Period/Parameters	*1910-2014 tau*	*1910-2014 p-value*	*1910-2014 Percent of median*	*1910-2014 Median*	*1925-2014 tau*	*1925-2014 p-value*	*1925-2014 Percent of median*	*1925-2014 Median*	*1950-2014 tau*	*1950-2014 p-value*	*1950-2014 Percent of median*	*1950-2014 Median*	*1985-2014 tau*	*1985-2014 p-value*	*1985-2014 Percent of median*	*1985-2014 Median*
Annual																
Precipitation	0.06	0.39	0.07	45.36	0.00	0.95	-0.01	46.17	-0.18	0.03	-0.35	47.43	0.03	0.838	0.17	43.88
Max Temperature	0.37	0.00	0.04	59.84	0.24	0.00	0.03	60.13	0.40	0.00	0.06	60.39	-0.13	0.323	-0.03	61.13
Average Temperature	0.33	0.00	0.03	52.73	0.16	0.03	0.01	52.90	0.32	0.00	0.04	52.87	-0.37	0.005	-0.09	53.32
Min Temperature	0.17	0.01	0.02	45.47	0.00	0.99	0.00	45.60	0.09	0.30	0.01	45.57	-0.33	0.010	-0.13	45.88
Winter																
Precipitation	0.02	0.72	0.05	22.25	0.02	0.83	0.05	22.70	-0.10	0.26	-0.29	23.01	-0.08	0.571	-0.67	22.86
Max Temperature	0.23	0.00	0.04	53.61	0.11	0.12	0.03	53.96	0.24	0.00	0.08	53.89	-0.15	0.256	-0.07	54.96
Average Temperature	0.18	0.01	0.03	47.05	0.04	0.60	0.01	47.34	0.19	0.02	0.05	47.28	-0.20	0.117	-0.13	47.75
Min Temperature	0.00	0.96	0.00	40.72	-0.09	0.21	-0.03	40.75	-0.01	0.92	0.00	40.68	-0.28	0.031	-0.19	40.88
Spring																
Precipitation	0.08	0.24	0.18	10.78	0.02	0.83	0.04	11.18	-0.01	0.90	-0.04	10.60	-0.06	0.669	-0.38	10.75
Max Temperature	0.25	0.00	0.04	57.65	0.16	0.02	0.03	57.80	0.37	0.00	0.09	57.88	-0.15	0.255	-0.08	59.18
Average Temperature	0.22	0.00	0.03	50.65	0.09	0.19	0.02	50.75	0.34	0.00	0.07	50.70	-0.31	0.020	-0.14	51.63
Min Temperature	0.08	0.24	0.01	43.71	-0.02	0.77	0.00	43.78	0.14	0.09	0.04	43.72	-0.30	0.022	-0.19	44.27
Summer																
Precipitation	0.07	0.31	0.22	0.93	0.07	0.33	0.29	0.90	0.03	0.75	0.14	1.00	0.00	0.985	0.09	0.70
Max Temperature	0.31	0.00	0.03	65.79	0.23	0.00	0.02	65.94	0.33	0.00	0.05	65.92	-0.28	0.033	-0.10	67.33
Average Temperature	0.39	0.00	0.03	58.59	0.25	0.00	0.02	58.75	0.37	0.00	0.04	58.76	-0.36	0.006	-0.08	59.62
Min Temperature	0.30	0.00	0.03	51.39	0.15	0.03	0.02	51.45	0.22	0.01	0.03	51.52	-0.18	0.172	-0.07	51.78
Fall																
Precipitation	-0.02	0.80	-0.04	9.33	-0.07	0.33	-0.22	9.49	-0.19	0.02	-0.87	9.93	-0.01	0.956	-0.03	8.34
Max Temperature	0.23	0.00	0.02	62.80	0.17	0.02	0.02	62.88	0.13	0.14	0.02	63.12	0.04	0.780	0.01	63.20
Average Temperature	0.24	0.00	0.02	54.65	0.10	0.16	0.01	54.85	-0.03	0.75	0.00	54.88	-0.24	0.075	-0.06	54.94
Min Temperature	0.12	0.06	0.02	46.54	-0.03	0.70	0.00	46.64	-0.14	0.10	-0.03	46.63	-0.27	0.044	-0.11	46.55
Cool Season																
Precipitation	0.04	0.56	0.09	18.86	-0.02	0.76	-0.06	19.43	-0.13	0.13	-0.39	19.89	-0.08	0.571	-0.71	18.12
Max Temperature	0.32	0.00	0.03	62.62	0.22	0.00	0.02	62.74	0.24	0.00	0.03	62.93	-0.17	0.201	-0.06	63.26
Average Temperature	0.33	0.00	0.02	55.01	0.16	0.02	0.01	55.16	0.16	0.06	0.02	55.25	-0.27	0.038	-0.06	55.43
Min Temperature	0.18	0.01	0.02	47.35	0.02	0.83	0.00	47.53	-0.04	0.62	-0.01	47.55	-0.27	0.038	-0.09	47.62
January																
Precipitation	-0.04	0.60	-0.10	7.61	-0.01	0.93	-0.03	7.44	-0.20	0.02	-0.90	8.00	-0.09	0.491	-1.09	7.14
Max Temperature	0.21	0.00	0.06	53.45	0.16	0.03	0.05	53.63	0.29	0.00	0.13	53.35	-0.10	0.468	-0.07	54.98
Average Temperature	0.18	0.01	0.04	46.64	0.14	0.06	0.04	46.81	0.32	0.00	0.12	46.62	-0.14	0.305	-0.12	47.73
Min Temperature	0.00	0.95	0.00	40.12	-0.03	0.68	-0.01	40.12	0.09	0.30	0.06	39.62	-0.17	0.211	-0.20	40.48
February																
Precipitation	-0.03	0.65	-0.09	6.23	-0.03	0.70	-0.09	6.02	-0.06	0.47	-0.32	6.04	-0.02	0.896	-0.33	5.43
Max Temperature	0.23	0.00	0.06	53.92	0.12	0.09	0.03	54.55	0.20	0.02	0.09	54.40	-0.11	0.402	-0.06	56.35
Average Temperature	0.21	0.00	0.04	47.29	0.07	0.34	0.02	47.77	0.17	0.05	0.06	47.81	-0.20	0.139	-0.13	48.12
Min Temperature	0.04	0.57	0.01	40.91	-0.04	0.54	-0.02	41.00	0.04	0.60	0.02	40.62	-0.25	0.063	-0.32	40.65
March																
Precipitation	0.09	0.16	0.24	5.97	0.03	0.67	0.11	6.09	-0.08	0.38	-0.31	6.24	-0.11	0.402	-1.28	5.58
Max Temperature	0.22	0.00	0.05	54.82	0.18	0.01	0.05	55.25	0.36	0.00	0.13	55.21	-0.08	0.539	-0.07	56.92
Average Temperature	0.22	0.00	0.04	48.24	0.15	0.03	0.03	48.45	0.40	0.00	0.10	48.26	-0.19	0.150	-0.11	49.21
Min Temperature	0.08	0.22	0.02	41.12	0.04	0.58	0.01	41.28	0.14	0.11	0.07	41.16	-0.26	0.053	-0.28	41.77

Time Period/Parameters	*1910-2014 tau*	*1910-2014 p-value*	*1910-2014 Percent of median*	*1910-2014 Median*	*1925-2014 tau*	*1925-2014 p-value*	*1925-2014 Percent of median*	*1925-2014 Median*	*1950-2014 tau*	*1950-2014 p-value*	*1950-2014 Percent of median*	*1950-2014 Median*	*1985-2014 tau*	*1985-2014 p-value*	*1985-2014 Percent of median*	*1985-2014 Median*
April																
Precipitation	0.01	0.86	0.04	3.17	0.01	0.89	0.03	3.12	0.05	0.56	0.26	3.17	0.14	0.305	1.54	2.83
Max Temperature	0.19	0.00	0.03	57.36	0.13	0.07	0.02	57.46	0.32	0.00	0.08	57.45	-0.21	0.120	-0.09	58.34
Average Temperature	0.11	0.10	0.02	50.19	0.01	0.84	0.00	50.28	0.25	0.00	0.05	50.25	-0.38	0.003	-0.18	51.08
Min Temperature	-0.01	0.85	0.00	43.14	-0.09	0.21	-0.02	43.24	0.08	0.38	0.02	43.03	-0.33	0.013	-0.20	43.54
May																
Precipitation	0.03	0.66	0.11	1.48	-0.01	0.88	-0.05	1.55	0.03	0.69	0.17	1.48	-0.12	0.381	-1.82	1.55
Max Temperature	0.22	0.00	0.04	60.67	0.10	0.15	0.02	61.01	0.24	0.00	0.07	61.18	-0.20	0.139	-0.11	62.37
Average Temperature	0.21	0.00	0.03	53.46	0.05	0.49	0.01	53.73	0.27	0.00	0.05	53.54	-0.17	0.211	-0.09	54.57
Min Temperature	0.10	0.12	0.02	46.38	-0.03	0.73	0.00	46.57	0.12	0.18	0.03	46.26	-0.15	0.255	-0.08	46.68
June																
Precipitation	0.01	0.91	0.03	0.46	0.00	0.97	0.01	0.46	0.02	0.79	0.20	0.45	-0.01	0.956	-0.23	0.46
Max Temperature	0.19	0.00	0.02	63.98	0.11	0.12	0.02	64.22	0.25	0.00	0.06	64.23	-0.13	0.323	-0.06	64.55
Average Temperature	0.21	0.00	0.02	56.98	0.06	0.44	0.01	57.10	0.21	0.01	0.04	57.02	-0.24	0.069	-0.08	57.26
Min Temperature	0.16	0.02	0.02	49.92	0.01	0.92	0.00	49.98	0.11	0.19	0.02	49.95	-0.18	0.185	-0.08	50.30
July																
Precipitation	0.16	0.02	0.79	0.04	0.15	0.04	0.84	0.05	0.13	0.13	0.87	0.05	-0.18	0.185	-4.24	0.06
Max Temperature	0.30	0.00	0.03	66.34	0.20	0.01	0.03	66.72	0.30	0.00	0.06	66.74	-0.35	0.007	-0.14	68.05
Average Temperature	0.36	0.00	0.03	59.15	0.23	0.00	0.03	59.24	0.38	0.00	0.06	59.23	-0.27	0.044	-0.10	60.42
Min Temperature	0.26	0.00	0.03	51.78	0.15	0.03	0.02	51.88	0.23	0.01	0.04	52.01	-0.09	0.515	-0.05	52.25
August																
Precipitation	0.15	0.02	0.67	0.05	0.14	0.05	0.84	0.06	0.01	0.89	0.02	0.07	0.02	0.895	0.03	0.09
Max Temperature	0.28	0.00	0.03	67.19	0.24	0.00	0.03	67.25	0.20	0.02	0.04	67.86	-0.30	0.022	-0.09	68.60
Average Temperature	0.36	0.00	0.03	59.91	0.26	0.00	0.03	60.01	0.22	0.01	0.03	60.23	-0.25	0.063	-0.09	60.48
Min Temperature	0.27	0.00	0.04	52.12	0.16	0.03	0.03	52.62	0.12	0.16	0.03	52.72	-0.14	0.305	-0.07	52.83
September																
Precipitation	-0.10	0.13	-0.45	0.59	-0.08	0.28	-0.36	0.61	-0.13	0.13	-1.18	0.56	0.01	0.956	0.12	0.35
Max Temperature	0.16	0.01	0.02	67.43	0.15	0.03	0.02	67.48	0.07	0.42	0.02	67.60	0.04	0.780	0.02	67.52
Average Temperature	0.26	0.00	0.03	58.65	0.16	0.02	0.02	58.96	0.04	0.61	0.01	59.21	0.02	0.896	0.01	59.24
Min Temperature	0.20	0.00	0.03	50.20	0.08	0.28	0.01	50.39	-0.06	0.48	-0.01	50.37	-0.09	0.491	-0.05	49.99
October																
Precipitation	-0.01	0.88	-0.03	2.41	-0.09	0.22	-0.40	2.49	-0.15	0.08	-0.90	2.41	-0.04	0.752	-0.71	2.00
Max Temperature	0.21	0.00	0.03	63.50	0.14	0.06	0.02	63.66	0.10	0.25	0.02	63.78	0.00	0.985	-0.01	63.74
Average Temperature	0.19	0.00	0.02	55.09	0.06	0.44	0.01	55.46	-0.01	0.94	0.00	55.54	-0.30	0.025	-0.09	55.59
Min Temperature	0.06	0.37	0.01	46.63	-0.07	0.34	-0.01	46.73	-0.10	0.24	-0.03	46.66	-0.30	0.025	-0.19	46.66
November																
Precipitation	-0.02	0.73	-0.08	5.89	-0.04	0.62	-0.16	5.47	-0.14	0.09	-0.78	6.13	-0.03	0.838	-0.34	4.45
Max Temperature	0.11	0.10	0.02	57.35	0.07	0.32	0.02	57.41	0.09	0.28	0.03	57.56	0.03	0.809	0.03	57.72
Average Temperature	0.09	0.17	0.01	49.96	0.01	0.93	0.00	50.35	-0.03	0.70	-0.01	50.36	-0.02	0.896	-0.02	50.35
Min Temperature	0.02	0.73	0.01	43.03	-0.05	0.51	-0.02	43.12	-0.12	0.15	-0.06	43.38	-0.11	0.423	-0.16	42.99
December																
Precipitation	0.03	0.60	0.10	7.46	-0.01	0.90	-0.03	8.11	-0.05	0.54	-0.24	8.35	-0.03	0.809	-0.68	7.97
Max Temperature	0.14	0.03	0.03	53.76	0.05	0.49	0.01	53.99	0.14	0.10	0.05	53.93	0.05	0.724	0.02	54.23
Average Temperature	0.05	0.41	0.01	47.19	-0.09	0.23	-0.02	47.33	-0.02	0.82	-0.01	47.19	-0.04	0.780	-0.04	47.23
Min Temperature	-0.03	0.62	-0.01	40.65	-0.12	0.09	-0.05	40.73	-0.09	0.31	-0.05	40.29	-0.09	0.515	-0.11	39.59

Key: p-Value = probability level; tau = Kendall's tau

Notes: Precipitation is measured in inches, temperature is measured in degrees Fahrenheit

Results shaded in blue are statistically significant wetter/cooler trends (upward trends in precipitation and downward trends in temperature) at a p-value of 0.05

Results shaded in red are statistically significant warmer/drier trends (downward trends in precipitation and upward trends in temperature) at a p-value of 0.05

Table B4. Results of time-series trend analysis of annual and seasonal precipitation and temperature at the Scotia Climate Station (CDEC SCA)

Time Period/Parameters	*1925-2014 tau*	*1925-2014 p-value*	*1925-2014 Percent of median*	*1925-2014 Median*	*1950-2014 tau*	*1950-2014 p-value*	*1950-2014 Percent of median*	*1950-2014 Median*	*1985-2014 tau*	*1985-2014 p-value*	*1985-2014 Percent of median*	*1985-2014 Median*
Annual Precipitation	0.01	0.85	0.02	46.81	-0.17	0.05	-0.33	48.05	0.09	0.501	0.46	45.64
Winter Precipitation	-0.02	0.79	-0.05	23.47	-0.10	0.24	-0.34	24.06	-0.03	0.840	-0.25	23.47
Spring Precipitation	0.07	0.37	0.21	10.20	0.03	0.76	0.11	10.46	0.02	0.858	0.39	10.30
Summer Precipitation	0.00	0.99	0.00	0.67	-0.02	0.81	-0.15	0.72	-0.08	0.539	-0.72	0.69
Fall Precipitation	-0.03	0.71	-0.09	9.06	-0.15	0.08	-0.56	9.12	0.12	0.376	0.90	7.92
Cool Season Precipitation	0.03	0.70			-0.06	0.51	-0.16	18.98	0.09	0.501	0.71	17.38
January Precipitation	-0.04	0.55	-0.18	7.58	-0.19	0.03	-1.10	8.21	-0.03	0.860	-0.47	6.76
February Precipitation	0.00	0.97	0.01	6.65	-0.05	0.59	-0.25	6.73	0.01	0.943	0.25	5.76
March Precipitation	0.07	0.34	0.25	6.10	0.01	0.92	0.03	6.15	0.01	0.972	0.04	6.00
April Precipitation	0.06	0.42	0.22	3.17	0.07	0.41	0.29	3.22	0.17	0.197	1.86	2.71
May Precipitation	0.04	0.57	0.23	1.40	0.05	0.55	0.31	1.37	-0.14	0.305	-1.66	1.59
June Precipitation	-0.05	0.52	-0.30	0.35	0.02	0.78	0.19	0.28	-0.05	0.680	-0.90	0.35
July Precipitation	0.20	0.01	0.91	0.02	0.02	0.84	0.00	0.03	-0.26	0.057	-4.76	0.03
August Precipitation	0.12	0.13	0.00	0.03	-0.08	0.38	0.00	0.05	-0.09	0.513	0.00	0.02
September Precipitation	0.02	0.75	0.00	0.31	-0.01	0.87	0.00	0.30	0.14	0.296	3.02	0.26
October Precipitation	-0.03	0.66	-0.18	2.24	-0.06	0.50	-0.34	2.27	0.07	0.620	0.67	2.16
November Precipitation	0.00	0.97	-0.01	5.42	-0.10	0.22	-0.55	5.52	0.05	0.724	0.31	4.70
December Precipitation	0.00	0.99	0.01	8.00	0.00	0.97	0.02	7.85	0.07	0.592	0.93	8.84

Key: p-Value = probability level; tau = Kendall's tau

Notes:

Precipitation is measured in inches, temperature is measured in degrees Fahrenheit

Results shaded in blue are statistically significant wetter/cooler trends (upward trends in precipitation and downward trends in temperature) at a p-value of 0.05

Results shaded in red are statistically significant warmer/drier trends (downward trends in precipitation and upward trends in temperature) at a p-value of 0.05